Chapter 8
Polypropylene Blends: Properties Control by Design

Wen Shyang Chow

Contents

W. S. Chow (✉)
School of Materials and Mineral Resources Engineering, Universiti Sains Malaysia, Engineering Campus, 14300 Nibong Tebal, Penang, Malaysia
e-mail: shyang@usm.my

J. Karger-Kocsis and T. Bárány (eds.), *Polypropylene Handbook*,
https://doi.org/10.1007/978-3-030-12903-3_8

Abstract This chapter focused on the structure-property-processing relationship of polypropylene blends (PP binary and ternary blends). The topics covers PP/thermoplastic, PP/elastomer, PP/thermoset, PP/recycled polymer and all-PP blends. The toughening, crystallization and compatibilization strategies for PP blends are summarized. The processing techniques and properties (e.g. rheology, foamability, dyeability, etc.) of PP blends are discussed. Some of the ways of properties optimization, modeling of flow behavior and molecular simulation are documented. This chapter ends with a future trend and prospective of the PP blends based materials.

8.1 Introduction

Polypropylene (PP) is widely used in automotive and packaging applications. It is undoubtly that PP is a versatile commodity plastic, which offers outstanding chemical and moisture resistance, low density, good processability and relatively low cost [1]. However, one of the limitations of PP is its poor impact toughness, especially at low temperature. One of the conventional approaches for overcoming this drawback is blending PP with elastomer and olefinic copolymer [2]. Polymer blending is an important technique in industrial practice, because it is an economically viable and versatile way of modifying some basic properties of existing polymers. The usual impact modifiers for the PP are olefinic copolymers based on ethylene and propylene, as well as styrenic rubber block copolymers [3]. The automotive application of polymers blends and reinforced polymers is a very rapidly increasing area. In the last decade the importance of PP and its blends have been increasing especially in bumpers, seating, dashboard, car interior and exterior trim and lighting applications. Development of mat-reinforced PP will profit from the availability of new metallocene-type PP resins [4]. Growing demand from end-use industries such as packaging, automotive and consumer products are expected to drive the market of PP blends.

PP is a polymorphic material which has at least three crystalline forms: α, β and γ. Commercial grades of PP crystallize essentially into the α-crystalline form under the usual industrial thermal conditions. The β-form can be obtained with the help of

a selective β-nucleating agent. The β-crystalline form has many performance characteristics, such as improved impact strength, in comparison with the traditional α-crystalline form. Hence, the research and development of β-PP-based blends would bring the benefits to improve the mechanical properties of PP [5].

Most of the PP blends (e.g. PP/thermoplastic, PP/elastomer, PP/thermoset) are incompatible, and thus they need suitable compatibilizer to stabilize their morphology and to strengthen their properties. Accordingly, some good examples of compatibilization system are discussed in the following section. In this chapter, the PP blends is mostly focus on PP as major matrix, so we can get a clearer picture to improve the properties of PP and its blends.

8.2 Basic Principles of Polymer Blends

Polymer blends offer a balance in mechanical and thermodynamical properties which are both unique and attractive for many industrial applications. They represent one of the most rapidly growing areas in polymer material science. Application of polymer blends in numerous fields such as automotive and packaging, designs of composite and biocompatible materials requires a fundamental understanding of the structure, phase state and composition of blends in the vicinity of interacting surfaces [6]. Polymer blends are either homogeneous or heterogeneous. In homogeneous blends, the final properties are often an arithmetic average of the properties of the blend components. In heterogeneous blends, the properties of all blend components are present. In general, practical use requires polymer blends which are partially or completely miscible.

Homogeneous miscibility in polymer blends requires a negative free energy of mixing that is $\Delta G_{mix} < 0$ (Eq. 8.1).

$$\Delta G_{mix} = \Delta H_{mix} - T \cdot \Delta S_{mix}, \tag{8.1}$$

where ΔH_{mix} is the enthalpy of mixing, ΔS_{mix} is the entropy of mixing, T is the temperature.

However, if two high molecular weight polymers are blended, the gain in entropy, ΔS_{mix} is negligible, and the free energy of mixing can only be negative if the heat of mixing, ΔH_{mix} is negative. In other words, the mixing must be exothermic, which requires specific interactions between the blend components. These interactions may range from strongly ionic to weak and nonbonding interactions, such as hydrogen bonding, ion-dipole, dipole-dipole and donor acceptor interactions. Usually, only van der Waals interactions occur, which explains why polymer miscibility is the exception rather than the rule. Examples of fully immiscible blends are PP/polyamide (PA), PA/acrylonitrile butadiene styrene (ABS), PA/ethylene-propylene-diene monomer (EPDM). All of these blends have become commercially successful, but only after being efficiently compatibilized [7].

The first and simplest, statistical thermodynamics model of polymer blends was developed by Flory and Huggins. The entropy of mixing, ΔS_{mix}, is assumed to be purely combinatorial and is calculated by enumerating the number of arrangements of the molecules on a lattice. The enthalpy, ΔH_{mix}, is simply the van der Waals energy of contact, and the difference between like and unlike pairs is summarized into a single term, the Flory–Huggins interaction parameter, χ, which varies linearly with inverse temperature so long as the interaction energy itself is temperature independent [8].

According to Flory–Huggins equation (Eq. 8.2):

$$\Delta G_{mix}/RT = \varphi_1 \ln(\varphi_1)/N_1 + \varphi_2 \ln(\varphi_2)/N_2 + \chi_{12}\varphi_1\varphi_2, \tag{8.2}$$

where ΔG_{mix} is the change of free energy on mixing two polymers, R is the gas constant, T is the temperature, φ_1 and φ_2 are the volume fractions and N_1 and N_2 are the segment numbers of the two blend components, respectively, and χ_{12} is the Flory–Huggins interaction parameter. When two high molecular weight polymers are blended, the gain in entropy, $\varphi_1\ln(\varphi_1)/N_1 + \varphi_2\ln(\varphi_2)/N_2$, is quite small, and the free energy of mixing, ΔG_{mix}, can be negative only if the heat of mixing is near zero or negative, $\chi_{12} < \sim 0.002$ [9].

In general, three different types of blends can be distinguished. In a completely miscible blend, for which $\chi_{12} < \sim 0.002$, it exhibits only one glass transition temperature (T_g), between the T_g values of the blend components, and in a close relation to the blend composition. In a partially miscible blend, a part of one component is dissolved in the other. As a result, two phases are observed, one phase rich in one component and the other phase rich in the other component. Each phase exhibits a T_g, which is between the T_g values of the pure components. In this case, the interphase is wide and interfacial adhesion is good. This type of blend is often referred to as compatible which exhibits satisfactory properties. By far most blends are fully immiscible. They demonstrate coarse phase morphology, with a sharp interphase, and the adhesion between the phases is poor, each components exhibit the T_g of the pure components [9].

One of the approaches for the quantitative estimation of interactions is the measurement of solvent absorption in the components and the blends [10]. The Flory–Huggins interaction parameter can be calculated from equilibrium solvent uptake by Eq. 8.3.

$$\ln a_1 = \ln \varphi_1 + (1 - \varphi_1) + (\chi_{12}\varphi_2 + \chi_{13}\varphi_3)(1 - \varphi_1) - \chi'_{23}\varphi_2\varphi_3, \tag{8.3}$$

where a_1 is the activity of the solvent, φ_1 is volume fraction in the blend at equilibrium, while χ_{12} and χ_{13} are the interaction parameters of the two-component solvent/polymer systems. χ'_{23} is related to the polymer/polymer interaction parameter by Eq. 8.4.

$$\chi'_{23} = \chi_{23}(V_1/V_2), \tag{8.4}$$

where V_1 and V_2 are the molar volumes of the solvent and polymer 2, respectively.

According to Imre et al. [10], the interactions and miscibility are closely related to structure and mechanical properties. A model developed earlier first for particulate filled polymers then adapted to blends allows the determination of a parameter associated to interaction. According to the model the composition dependence of tensile strength can be expressed as shown by Eq. 8.5.

$$\sigma_T = \sigma_{To}\lambda^n[(1-\varphi_d)/(1+2.5\varphi_d)]\exp(B_T\varphi_d), \tag{8.5}$$

where σ_T and σ_{To} are the true tensile strength ($\sigma_T = \sigma\lambda$, $\lambda = L/L_o$) of the heterogeneous polymeric system (blend or composite) and the matrix respectively, n is a parameter expressing the strain hardening characteristics of the matrix, and B is related to the load bearing capacity of the dispersed phase. This latter is determined by interactions as well as by the inherent properties of the components as expressed by Eq. 8.6.

$$B = \ln[(C(\sigma_{Td}/\sigma_{To})], \tag{8.6}$$

where σ_{Td} is the strength of the dispersed phase, while C is related to stress transfer between the phases, i.e. interactions, and was found to correlate inversely with the Flory–Huggins interaction parameter. According to the model, plotting a natural logarithm of reduced tensile strength $[\sigma_{Tred} = \sigma_T(1 + 2.5\varphi)/\lambda^n/(1-\varphi)]$ against composition should obtain a straight line, the slope of which is parameter B and from that parameter C can be calculated.

Nanoblend is one of the future directions in designing polymer blending. Nanostructured polymer blends (referred to as polymer nanoblends) are polymeric systems in which the dispersed-phase domains exhibit length scales of 100 nm or less. Nanoblends have been developed to be applied in electronic, membrane, sensing probes and optical applications. There are several approaches to obtain nanoblends, e.g. reactive extrusion, in situ polymerization, solution casting and melt blending. Polymer nanoblends can be designed by two approaches, one considering thermodynamics aspects and the other one considering micro-rheology basis. In terms of the thermodynamics aspects, the interaction energy density parameter can be used to predict polymer blends phase separation with disperse domains. The interaction energy density parameter is related to the Flory–Huggins interaction parameter and depends on the polymers solubility parameters. Nanostructured blends can be obtained by choosing adequate micro-rheological parameters for the blend such as: disperse and matrix phases viscosity ratio; shear and extensional flow conditions and interfacial tension or energy. All those parameters affect the final particle size of the blend disperse phase. In addition, sometimes compatibilization is necessary to reduce the interfacial tension and to prevent the coalescence for higher disperse phase content in the polymer blend [11]. One of main rheological parameters is the viscosity ratio between the liquids, which can be determined by Eq. 8.7.

$$\eta_r = \eta_d/\eta_m, \tag{8.7}$$

where η_d and η_m are the viscosity values for the disperse and matrix phase at the mixing temperature, respectively. For simple shear flow at small Newtonian liquid deformations, the particle diameter D, due the drop breakup, can be determined by balancing interfacial tension (Γ) and shear forces ($\dot{\gamma}\eta_m$), as shown in Eq. 8.8:

$$D = 4\Gamma(\eta_r + 1)/[\dot{\gamma}\eta_m((19/4)\eta_r + 4)], \tag{8.8}$$

where $\gamma^{\cdot}$ is the shear rate and η_m is the matrix phase viscosity.

According to Costa et al. [11], the Eq. 8.8 has been further modified to represent drop breakup in polymer blends, together with the consideration of viscoelastic effects. It was established a critical capillary number value, C_{acrit}, above which drop breakup for polymer blends will occur leading to disperse particle diameter size D, estimated by Eq. 8.9:

$$D > (2\Gamma C_{acrit}/[\eta_m\dot{\gamma} - N_1]), \tag{8.9}$$

where, N_1 represents the first normal stress difference due to the elastic forces during polymer mixing. C_{acrit} can be estimated as approximately 0.5 for $0.1 < \eta_r < 1$. By optimizing shear and extensional flow conditions and reducing as much as possible the interfacial energy, Γ, it is possible to obtain disperse particle size in the range of nanoscale. In addition, it is necessary to prevent as much as possible the particles coalescence, which can be done through compatibilization and for lower contents of the disperse phase component.

There are several strategies can be used to improve the interaction and compatibility of the polymer blends, for example, addition of premade grafted and block copolymers, addition of reactive polymers, interchange reactions, addition of ionomers, reactive compatibilization and etc. Recently, it was also reported that nanoparticles can act as compatibilizers provided that they can ensure a strong interfacial adhesion between two incompatible polymers [12].

8.3 PP Binary Blends

8.3.1 PP/Thermoplastic Blends

PP has been blended with other thermoplastic to obtain desired properties, with the aim to combine the advantages of the individual polymers in the blends. Plently of PP blends are reported, for example, PP/polyamide (PA), PP/polystyrene (PS), PP/polycarbonate (PC), PP/poly(methyl methacrylate) (PMMA), PP/polyethylene (PE), PP/poly(ethylene terephthalate) (PET), PP/liquid crystalline polymer (LCP) and so on. In this chapter, a few examples of the PP/thermoplastics blends are discussed.

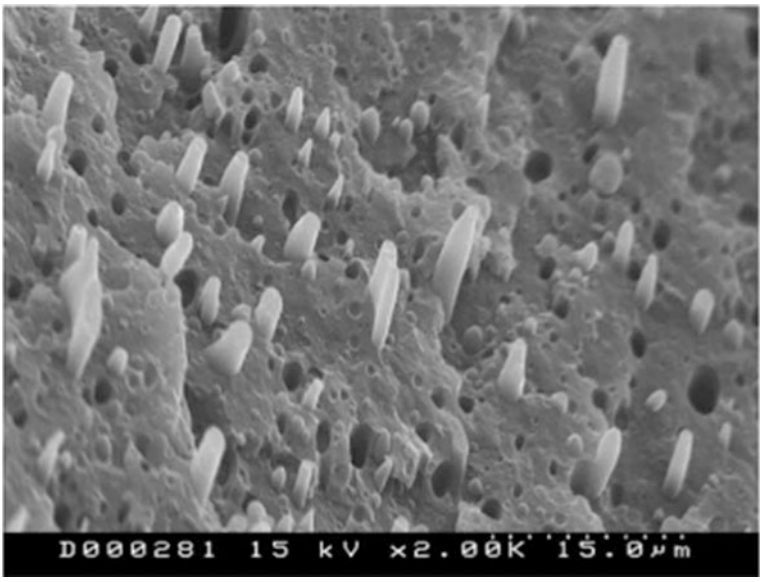

Fig. 8.1 SEM micrograph of PP/PA12 (75/25) blends taken with incidence angle of 40°. Adapted from Aranburu and Eguiazábal [14], with the permission of Hindawi Publishing Corporation

8.3.1.1 PP/PA Blends

Polyamide 6 and PP blending has been attempted to achieve improvement in mechanical properties, paintability and barrier properties, where PA6 contribute mechanical and thermal properties, while PP ensures good processability and insensitivity to moisture [13]. Aranburu and Eguiazábal [14] studied the mechanical and morphological properties of PP/PA12 blends. Figure 8.1 shows the SEM micrograph of PP/PA12 (75/25) blends taken with incidence angle of 40°. It was found that the PA12 particles are elongated in a direction parallel to the injection molding flow direction.

8.3.1.2 PP/PS Blends

PP blends with styrene polymers or copolymers attract much attention. To increase the rigidity of PP and improve toughness and solvent resistance of PS, the physical and mechanical properties, morphologies of PP/PS blends and compatibilized blends have been widely studied [15].

8.3.1.3 PP/Polyethylene Co-octene (POE)

Modified atmosphere packaging (MAP) is a passive way to create an appropriate gas composition around the product, which is typically packaged in plastic bags during shipping, storage and marketing. Blends of PP/polyethylene co-octene (POE) make them very attractive to be used for MAP of fresh products such as apple, blueberry and mushroom. For the maximum POE concentration used (40%), the oxygen permeability increased up to ~100% from that of neat PP. The addition of POE to PP was an effective way to prepare PP-based blends with enhanced oxygen and water vapour permeability [16].

8.3.1.4 PP/PET

PP/PET blend could be expected to combine the barrier properties of both components, since PET has a much lower permeability to gases and a higher permeability to water than PP. These two polymers are also complementary in their resistance to solvent and chemical attack. Since all these properties are of critical importance in packaging, this could be a potential application for these blends [17].

8.3.1.5 PP/LCP

Main chain liquid crystalline polymers (LCPs) have been used in thermoplastic blends to enhance processability (reduce viscosity) and to provide in situ reinforcement. This arises due to the tendency of low-viscosity main chain LCPs to readily fibrillate, particularly when deformed in an extensional flow field [18]. The modulus and tensile strength of PP/thermotropic LCP blends increased with draw ratio and the LCP content. This reinforcement was associated to their morphological transformation from spherical droplets to oriented and elongated microfibrils [19].

8.3.1.6 PP/Polysulfone

Polysulfone (PSU) and PP-based polymers are commercially used for ultrafiltration and microfiltration (polysulfone supported on a PP backing) applications such as extraction of insulin, polymer synthesis and effluent water recovery [20].

8.3.1.7 PP/PS Nanoblend

Nanoblends, in which dispersed-phase domains exhibit length scales of order 100 nm or less, are of growing interest attributed to the potential for enhanced properties. The use of a divinylbenzene (DVB) crosslinking agent and styrene (St) comonomer in the preparation of PP/PS nanoblends by diffusion and

polymerization of St in isotactic polypropylene (iPP) pellets is an effective way to stabilize the initial nanoscopic morphology of the PP/PS blends during subsequent melt processing. With relatively high amounts of benzoyl peroxide (BPO) and DVB, the nanosized PS domains almost kept their shape and size, and only simple aggregates of a few PS particles with an average size of 130 nm were observed after melt mixing of the PP/PS blends [21].

8.3.2 PP Thermoplastic Elastomer

Thermoplastic elastomers (TPEs) prepared from polymer blends may be categorized into two types based on rubber vulcanization, i.e. thermoplastic olefins (TPOs) and thermoplastic vulcanizates (TPVs). TPOs often refer to the blends without rubber vulcanization and plastics normally used are polyolefins, i.e. PP and PE. Vulcanization in the rubber phase of TPVs has to occur during melt blending between plastic and rubber through dynamic vulcanization.

8.3.2.1 TPO and PP/Rubber Blends

Öksüz and Eroğlu [22] had investigated the effects of the elastomers, i.e. ethylene-propylene-diene monomer (EPDM), ethylene vinyl acetate (EVA) and styrene-butadiene-styrene (SBS) on the mechanical properties of isotactic polypropylene (iPP). The impact strength increases as the elastomer content increases from 3 to 15 wt%. EPDM is the most effective elastomer for higher toughness values and is followed by EVA and SBS. The higher toughness values obtained for EPDM is due to two factors: (1) good adhesion between EPDM and iPP, and (2) the structure of EPDM is much more flexible than EVA and SBS.

The presence of even a small amount of ionic groups exerts a signficant effect on the physical properties of the polymer. The ionic groups present in the polymers interact to form strong intermolecular ionic aggregates, which increase the adhesion of plastic and form the interlocked network structure in rubber/plastic blends. Su et al. [23] studied the mechanical properties and morphological structures of blends based on Zn^{2+} neutralized low degree sulfated ethylene propylene diene monomer rubber (Zn–SEPDM) ionomer and PP. It was found that Zn^{2+} neutralized low degree sulfated EPDM ionomer and PP blends, which are new thermoplastic elastomeric materials, have better mechanical properties than those of PP/EPDM blend. Scanning electron microscopy (SEM) results confirmed that the finer dispersed phase sizes and the smaller interparticle distances are the main reasons for the improvement of the mechanical properties of PP/EPDM blends.

Chakraborty et al. [24] prepared a series of TPE from a binary blend of EPDM and iPP using different types of phase modifiers. The influence of sulphonated EPDM, maleated EPDM, styrene-ethylene-cobutylene-styrene block copolymer, maleated PP, and acrylated PP as phase modifiers showed improved

physico-mechanical properties (e.g. maximum stress, elongation at break, moduli and tension set).

Ma et al. [25] investigated the structure and morphology of partly compatible binary blends of PP with poly(*cis*-butadiene) rubber using SEM. Within the region of compositions from 50 to 70 wt% iPP, the blends show a co-continuous morphology, and the phase-inversion occurs in this region. Hristov et al. [26] studied the fracture toughness of PP/poly(styrene-*ran*-butadiene) rubber (SBR) blends as a function of concentration of maleic anhydride (MA) in the maleated polypropylene (MAPP) compatibilizer under uniaxial static and impact loading conditions. The addition of MAPP to the unmodified PP/rubber blend enhanced the tensile modulus and yield stress as well as the Charpy impact strength. The compatibilized materials deformed uniformly within the gauge length by intensive stress whitening during the uniaxial loading. Salmah et al. [27] prepared PP/chloroprene rubber (CR) blends and it was found that the elongation at break of the blends of PP was increased by the incorporation of CR.

8.3.2.2 TPV

Thermoplastic vulcanizates (TPVs) belong to the family of thermoplastic rubbers. They are (re)processed as thermoplastic resins but exhibits properties similar to those of traditional rubbers. TPVs that combine the processing advantages of thermoplastics with the functional performances of vulcanized rubber are a specific class of polymeric materials, prepared by high shear blending of in situ dynamically vulcanized rubber with a molten thermoplastic. The resulting blend has small, uniform, and finely distributed crosslinked rubber particle matrices. TPV grades are replacing rubbers in increasing amount in various applications, for example, automotive (e.g., windshield blades, glass sealing profiles, shock absorbers, expansion bellows, grips, handles and internal covers) attributed to the recyclability and reprocessability of TPV [28, 29]. PP/EPDM TPVs are available commercially, and have been recognized for their unique physical and mechanical properties as well as excellent weathering resistance over a range of blend combinations [30].

Karger-Kocsis et al. [31] conducted morphological study of PP/EPDM and PP/polyolefin thermoplastic vulcanizate blends. The differences in melt viscosities of the blended components were characterized by the phase viscosity ratio (μ). High degree of dispersion of the impact modifier can be achieved if melt viscosities of the blended components are very closely matched (when $\mu \backsimeq 1$). It was concluded from SEM results that, below an impact modifier content of 20 wt%, the modifier formed the dispersed phase in the continuous PP matrix. In blends containing 50 wt% of impact modifier, the latter may also form continuous phase depending on its type and μ value beside the still continuous PP phase (co-continuous network structure).

In numerous applications the TPV parts are exposed to service conditions where scratch and wear resistances are of great importance. Karger-Kocsis et al. [28] studied the friction, sliding and rolling wear characteristics of PP/EPDM TPV (Santoprene® grades) against steel counterparts in dry condition. The wear

performance of the TPVs was investigated in different tribotests, viz. pin-on-plate (POP), cylinder-on-plate (fretting) and rolling ball-on-plate (RBOP), whereby plate was always the rubber. It was established that increasing hardness caused by increasing amount of PP, is usually accompanied with reduced coefficient of friction (COF) and specific wear rate. Both of these proved to be highly dependent on the configuration and parameters of the related tribotests.

Jain et al. [32] examined the deformation and fracture behavior of several PP/EPDM TPV (EPDM; 10–40 wt%) and compared with those of uncrosslinked blends of PP/EPDM. The impact strength of the dynamic vulcanized PP/EPDM TPV blends is higher values compared with uncrosslinked blends. The nucleation effect of the crosslinked particles and the decrease of crystallinity of the EPDM rubber were considered as a contributing factor to the improvement in the impact strength.

Gupta et al. [33] prepared blends of PP/EPDM by dynamic vulcanization using dimethylol phenolic resin. A change in morphology from dispersed phase to co-continuous phase takes place in composition range of 30–40 wt% in unvulcanized blends and in composition range of 20–30 wt% in vulcanized blends. The dynamic vulcanization improved the plastic deformation and tensile properties significantly. The increase of interfacial adhesion caused by the three-dimensional network is considered to be the most important factor in the improvement.

Dynamic vulcanisation by electron induced reactive processing is a potential alternative to prepare TPV. Electron induced reactive processing is a novel technique where chemical reactions are induced by spatial and temporal precise energy input via high energy electrons under dynamic conditions of melt mixing. Naskar et al. [34] prepared TPV by dynamic vulcanisation with 50:50 blend ratio of PP and EPDM using novel electron induced reactive processing under various conditions as an alternative to conventional phenolic resin and peroxide cross-linking systems. Figure 8.2 shows schematic representation of the set-up for the coupling of an electron accelerator with an internal mixer. Their results indicated that in situ compatibilization of PP and EPDM, as well as crosslinking in the EPDM phase are occurring simultaneously, which contributing to the enhancement in the mechanical properties.

Tanrattanakul et al. [29] characterized TPE from PP and natural rubber (NR) with and without phenolic resin as a vulcanizing agent. The unvulcanized thermoplastic natural rubber (uTPNR) illustrated co-continuous phase morphology, whereas the vulcanized thermoplastic natural rubber (vTPNR) displayed dispersed phase of vulcanized natural rubber. Dynamic vulcanization improved tensile strength, elongation at break, tension set and degree of swelling of the TPEs. The vTPNR exhibited higher ozone resistance and swelling resistance than the uTPNR.

Nakason et al. [35] prepared TPV based on epoxidized natural rubber (ENR)/PP blends by dynamic vulcanization. It was found that the TPV prepared from ENR/PP with phenolic modified PP (Ph-PP) as a compatibilizer gave the highest mechanical properties. Another study from Nakason et al. [36] demonstrated that mixing torque, apparent shear stress, apparent shear viscosity, tensile strength, and hardness properties of ENR/PP TPV (with Ph-PP compatibilizer) increased with increasing

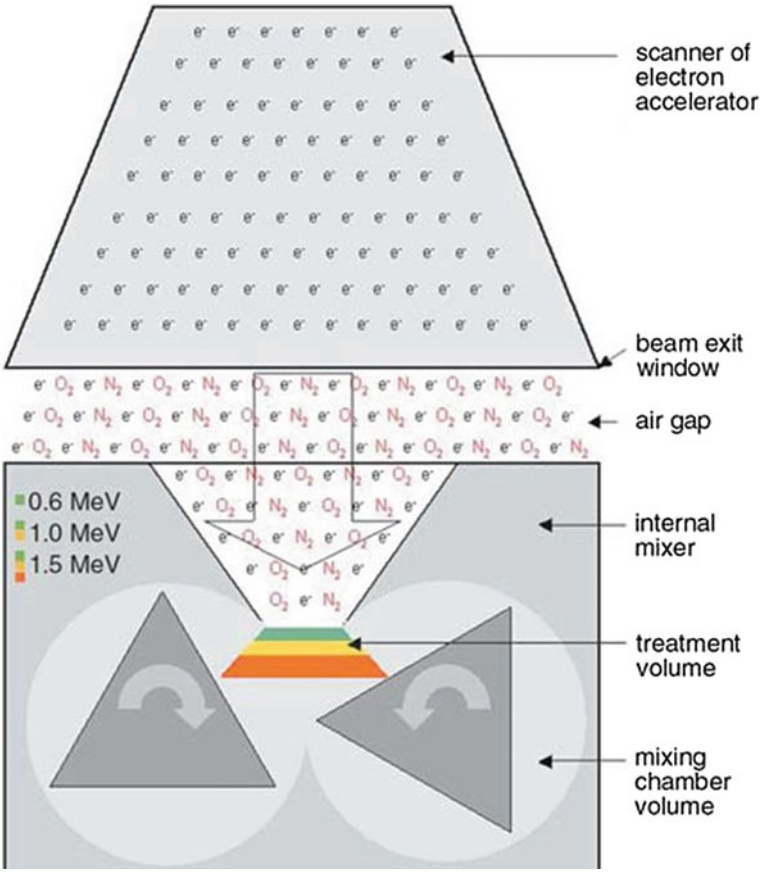

Fig. 8.2 Schematic representation of the set-up: coupling of an electron accelerator with an internal mixer. Adapted from Naskar et al. [34], with the permission of BME-PT

levels of epoxide groups in the ENR. This is attributed to increasing level of chemical interaction between the methylol groups of the Ph-PP and polar functional groups of the ENR.

A TPV composed of PP and EVA, was crosslinked by tetrapropoxysilane (TPOS) as crosslinking agent in the presence of dibutyl tin oxide (DBTO) as catalyst. The crosslinking reaction was carried out through a transesterification reaction between the ester groups of EVA and the alkoxysilane groups of TPOS. This chemistry is non-radical, and thus prevents the degradation of PP in comparison with crosslinking reactions using peroxides as initiator. From the gel content and morphology analysis, it was showed that the correlation between the evolution of the two phase blend morphology and the crosslinking reaction conversion was almost the same for the preparing of the TPV in the internal mixer and

twin-screw extruder. The phase inversion seems to take place at a gel content of around 60% [37].

TPE prepared by blending thermoplastic with nitrile rubber (NBR) has been received a lot of interest because of the combination of the oil-resistant property, the excellent mechanical properties and processing behavior. Soares et al. [38] investigated the efficiency of dicumyl peroxide (DCP) in combination with N,N′-m-phenylene-bismaleimide (BMI) as a crosslinking system for the PP/NBR TPV in the presence of compatibilizing agents (i.e., maleic anhydride-grafted-PP (PP-g-MA)/amino compound and glycidyl methacrylate-grafted-PP (PP-g-GMA) with or without amino compound). The compatibilization with PP-g-MA and XNBR as the coreactive functional groups was performed in the presence of a small amount of triethylene-tetramine (TETA) to impart the adhesion. The PP-g-MA/TETA/XNBR, PP-g-GMA/TETA/XNBR, and PP-g-GMA/XNBR are efficient compatibilizing systems, since they promote an improved tensile properties and compression set when compared with un-compatibilized blend. Van Dyke et al. [39] applied dynamic vulcanization to prepare thermoplastic elastomer blends of PP with chlorobutyl (CIIR) and NBR rubbers. The ultimate tensile strength and hardness values increase as the proportion of PP is increased, in the range of 0–50 wt% PP.

Different TPV were prepared from elastomeric chlorosulfonated polyethylene (CSM) and PP by applying dynamic vulcanization technique. It was revealed that CSM/PP TPV show substantial improvement in stress at ultimate tensile strength, hardness and thermal stabilities with the incorporation of PP [40].

Babu et al. [41] studied the influence of the three structurally different coagents, namely triallyl cyanurate (TAC), trimethylol propane triacrylate (TMPTA) and N,N′-m-phenylene dimaleimide (MPDM) on the thermal and rheological properties of TPV based on the PP and ethylene octene copolymer (EOC). Coagent assisted peroxide cured system affects the crystallizing behavior due to the various types of reactions taking place simultaneously. Generally, increase in dynamic functions is attributed to the improved crosslinking in the EOC phase and immobilization of the interface by compatibilizing efficiency of coagent. It can be concluded that the dual role of MPDM i.e. as a booster for peroxide and as a reactive compatibilizer assist to improve the properties in the solid as well as in the melt state.

8.3.3 PP/Thermoset Blends

Some of the PP/thermoset blends are worth mentioning. The introduction of thermoset improves the properties of PP and it widens the application window of PP blends. Many thermoplastic vulcanizate have been attributed to the dynamic vulcanization of elastomer in the molten thermoplastic. By using the same concept dynamic vulcanization have been applied to the preparation of thermoplastic/thermoset blends.

8.3.3.1 PP/Unsaturated Polyester Blends

Wan et al. [42] prepared melt blending of PP with a low molecular weight (MW) crosslinkable unsaturated polyester (UP) resin using a batch mixer and a twin-screw extruder in the presence of peroxide free radical initiator. The blends are also characterized by FTIR which strongly suggests that the presence of block or graft PP-UP structures that may enhance phase interaction and promote compatibility in the reacted PP/UP blends. Such blends are considered as suitable compatibilizers of PP/high MW thermoplastic polyester blends and as modifiers for low density extrusion foaming of similar blends. The different rheological properties of PP and UP can be adjusted by a peroxide initiated reaction during reactive melt blending to produce a finer and more uniform morphology containing crosslinked UP particles in a low viscosity PP matrix. Mixing efficiency, protocol of addition and residence time in the batch and continuous mixers was shown to affect the morphology and rheology of the blends, some of which showed suspension-like behavior, typical of thermoplastic vulcanizates.

8.3.3.2 PP/Epoxy Blends

Jiang et al. [43] used dynamic vulcanization process to prepare PP/epoxy blends. The blends had crosslinked epoxy resin particles finely dispersed in the PP matrix. Maleic anhydride grafted polypropylene (PP-g-MAH) was used as a compatibilizer. The increase in the torque at equilibrium for the PP/PP-g-MAH/epoxy blends indicated the reaction between maleic anhydride (MA) groups of PP-g-MAH and the epoxy resin. The torque at equilibrium of the dynamically cured PP/epoxy blends increased with increasing epoxy resin content. The PP/epoxy blends compatibilized with MAH-g-PP have finer domains than the PP/epoxy blends. The dynamically cured PP/epoxy blends (PP/PP-g-MAH/epoxy/2-ethylene-4-methane-imidazole curing agent (EMI-2,4)) exhibited higher flexural modulus than the PP/epoxy and PP/PP-g-MAH/epoxy blends.

8.3.3.3 PP/Novolac Blends

Dynamically cured PP/novolac blends were prepared in a mixing chamber (190 °C and 50 rpm) in the presence of hexamethylenetetramine (HMTA) curing agent and PP-g-MAH. The PP/novolac blends exhibited shear-thinning behavior. It was found that the compatibilization together with the dynamic cure could increase the viscosity and modulus because of the formation of a grafting polymer between the PP-g-MAH and the curing novolac resin [44].

8.3.4 All-PP Blends

In this section, the "all-PP blends" defined as the blending of PP with different tacticity (i.e., effects of stereochemistry), blending PP with functionalized PP (e.g. grafted PP), blending PP with bimodal molecular weight distribution, blending PP with linear and branched chain.

8.3.4.1 PP Blends with Different Tacticity

The stereochemistry of PP strongly influences its final properties through a variety of morphological factors such as crystallinity, lamellar structure, spherulitic macrostructure, and melting behavior. Blends of atactic PP (aPP) with either isotactic polypropylene (iPP) or syndiotactic PP (sPP) homopolymer can exhibit some unique mechanical properties, with the aPP acting as a softening agent. Phillips [45] examined the morphology of iPP/aPP and iPP/sPP blends by using optical microscopy. Comparisons of constant molecular weight iPP/aPP and iPP/sPP mixtures show that the iPP/aPP blend pair exhibits greater miscibility than the iPP/sPP pair.

8.3.4.2 PP/Functional PP Blends

In the study of Flores-Gallardo et al. [46], PP was functionalized with acrylic acid (AA) and styrene as a co-monomer by means of a radical-initiated melt-grafting reaction. The formation of polypropylene grafted with acrylic acid (PP-g-AA) and polypropylene grafted with acrylic acid and styrene (PP-g-AAst) was confirmed. Blends of PP with 0–100 wt% of PP-g-AA were prepared by melt mixing. The contact angles of water on cast-film surfaces of PP/PP-g-AA blends decreases with increasing modified polymer content and decreasing PP-g-AA molecular weight. Using styrene as a second monomer produced a noticeable increase in grafting degree with no significant change in melt index. An increase in crystallization temperature of PP was observed when AA monomers were grafted into PP and with increasing PP-g-AA content in the blend, probably caused by a nucleation effect of AA monomers that would improve the crystallization capability of PP.

Saffar et al. [47] investigated miscibility of a binary blend consisting of PP and PP-g-AA (with an acrylic acid content of 6 wt%). It was found that by using atomic force microscopy (AFM) and time-of-flight secondary-ion mass spectrometry (ToF-SIMS) chemical imaging, an accurate quantitative evaluation of the phases in the polymer blends can be obtained. AFM data effectively detected dispersed-phase domains corresponding to the PP-g-AA rich phase. The size of the domains increased from around 50 nm up to around 250 nm as the PP-g-AA content increased from 5 to 20 wt%.

8.3.4.3 Bimodal PP Blends

Bimodal polypropylene was prepared using three metallocene catalysts: rac-$Me_2Si(Ind)_2ZrCl_2$ (CAT-1), rac-$Et(Ind)_2ZrCl_2$ (CAT-2) and rac-Me_2Si(2-Me-benzoind)$_2ZrCl_2$ (CAT-3). The rac-$Et(Ind)_2ZrCl_2$ (CAT-2) and rac-Me_2Si(2-Me-benzoind)$_2ZrCl_2$ (CAT-3) were combined in different proportions (wt%/wt%) of (CAT-2/CAT-3) for obtaining a new PP with a bimodal molecular weight distribution. The polymers obtained were compared with those coming from melt mixing of two PP with different molecular weights in an extruder. Both methods allow obtaining bimodal PP, but polymer melt blending shows partial miscibility effects and less crystallinity while binary catalytic systems have several advantages such as intimate mixing of high and low molecular weight components (improved product quality), less process complexity, and higher cost effectiveness [48].

8.3.4.4 Linear and Branched PP Blends

Fang et al. [49] investigated the effect of blending a long-chain branched PP (LCB-PP) with a linear PP (L-PP) on the processability and properties of blown films. Adding an LCB-PP significantly improved the melt strength which leads to strain-hardening behaviour. From bubble stability tests, it was found that area in the stability map increased with LCB-PP content. However, the addition of LCB-PP reduced the mechanical strength of the blown films with a more pronounced impact on the mechanical strength in transverse direction (TD). The addition of long branches created a row nucleated lamellar structure for the blend films, which favoured orientation of the crystals blocks along machine direction (MD).

8.4 Recycled PP Blends

For the benefits of sustainable development, plastic recycling is one of the alternatives to extend the self-life of polymers and thus it can help to reduce carbon footprint. In this section, both of the recycled PP/other polymer blends and recycled polymer/PP blends are discussed.

8.4.1 Recycled PP/Other Polymer Blends

Miskolczi et al. [50] prepared blends of waste PP (from automotive and packaging sector) and polyamide (from automotive sector) in the presence of compatibilizer (polyalkenyl-poly-maleic-anhydride-amide, polyalkenyl-poly-maleic-anhydride-ester, and maleic-anhydride (MA)-grafted-low-polymer). The tensile and flexural

strength and modulus was improved by the using of compatibilizer. This evidences a possible approach to minimize the plastic waste and contribute to the sustainable development of the plastic industry. Garcia et al. [51] investigated the deformation behavior of a recycled PP/partially devulcanized rubber (85 wt%/15 wt%) using morphological analysis (2D via scanning electron microscopy while 3D via X-ray microtomography). It was established that blend composed by the dispersed rubbery phase with the highest devulcanization level presented the most refined morphology. Figures 8.3 and 8.4 shows the 3D microstructures of recycled PP/devulcanized rubber (85/15) sample and recycled PP/vulcanized rubber (85/15) sample respectively. It was found that the dispersed phase of the recycled PP/devulcanized rubber blend is finer compared to that of recycled PP/vulcanized rubber. This indicates that the devulcanization process facilitates the breakup of the rubber particles during the mixing.

8.4.2 PP/Recycled Polymer Blends

Blending of recycled polyethylene terephthalate (RPET) from waste bottles with PP was performed in an attempt to enhance the processability of RPET. This could recycle PET bottles together with their PP-based caps (RPET/PP ratio was varied at 95/5 and 90/10). The specimens containing low molecular weight PP were found to remain homogeneous regardless of compatibilizer and PP content in the RPET/PP blends [52].

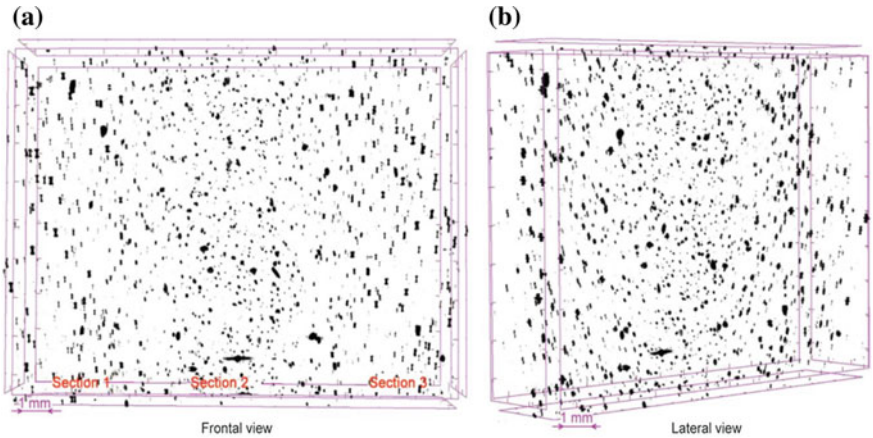

Fig. 8.3 3D images of the recycled PP/devulcanized rubber (85/15) sample using X-ray microtomography. Adapted from Garcia et al. [51], with permission of BME-PT. *Note* Devulcanized rubber prepared from vulcanized ground tire rubber treated in microwave for 6 min

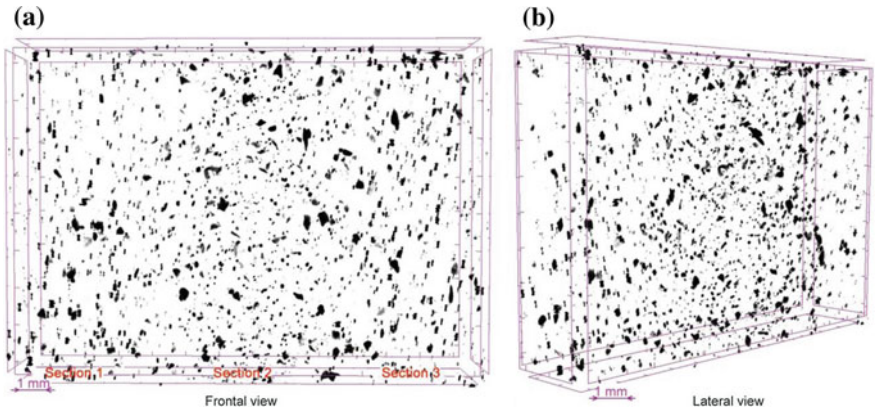

Fig. 8.4 3D images of the recycled PP/vulcanized rubber (85/15) sample using X-ray microtomography. Adapted from Garcia et al. [51], with permission of BME-PT

Polybutylene terephthalate (PBT) is extensively used for automotive and electronics applications. Mechanical recycling of this engineering plastics waste can be realized by blending polyolefins such as the PP. Potential advantages expected from blending the two components are as follows: low absorption of humidity, better processability, good thermal resistance, and dimensional stability. However, PP is neither miscible nor compatible with PBT due to a great difference in polarity. Compatibilization of polyester/polyolefin blends can be achieved by using suitable compatibilizers. Barhoumi et al. [53] prepared blends of recycled PBT parts obtained from scrapped cars (which are used in the electronic application, i.e. connector), and virgin PP by using twin-screw extruder at different compositions. Selected compositions were also prepared with the presence of ethylene-co-glycidyl methacrylate copolymer (E-GMA) and ethylene/methyl acrylate/glycidyl methacrylate terpolymer (E-MA-GMA) compatibilizers. Addition of E-GMA and E-MA-GMA to the PP/PBT blend exhibited a significant change in morphology and improved ductility because of interfacial reactions between PBT end chains and epoxy groups of GMA that generate EG-g-PBT copolymer. Moreover, thermal and viscoelastic study indicated that the miscibility of PP and PBT has been improved. The significant increase of the elongation at break of the PP/PBT/E-MA-GMA blends should be considered as a beneficial aspect.

Binary and ternary blends of the high viscosity recycled high-density polyethylene (reHDPE) from milk bottles, containing either homopolymer PP or copolymer PP, were developed in an effort to reduce viscosity and encourage ease of processing by injection molding, without a significant loss in mechanical properties [54]. Kazemi et al. [55] had reported that the addition of ethylene-octane copolymer (EOC) compatibilizer had improved deformability of recycled PP/PE blends.

Blending of PP with polyamide 6 (PA6) industrial wastes is an important way of valorization. In the presence of PP-g-MA compatibilizer, the interfacial adhesion

was improved, as a result of the creation of an interphase that was formed by the interaction between the PP-g-PA6 copolymer in situ and both phases. This interphase induced an improvement in tensile properties. From an application point of view, 20 wt% PA6 can be blended with PP without affecting Young's modulus and yield stress, however, reduction of elongation at break should be concerned [56].

8.5 PP Ternary Blends

PP ternary blends referring to the PP blends with (at least) another two polymers, for example, PP/PE/EPDM, PP/PA6/ABS, PP/PA/PS, PP/PET/PE and so on. In this section, a few examples of PP ternary blends are discussed.

Tchomakov et al. [57] investigated the ternary blends of high-density polyethylene (HDPE), EPDM and PP. It was found that the modulus, tensile strength and impact resistance can be improved by HDPE addition if the HDPE is localized within the EPDM phase. The use of a two-step mixing procedure where EPDM and PE were mixed together before their incorporation in the PP matrix resulted in finely dispersed droplets. This resulted in an additional 50% increase in Izod impact strength and more than a two-fold increase in elongation when compared to the standard one-step mixing. According to Vranjes and Rek [58] the PP/HDPE blend revealed poor adhesion between PP and HDPE phases. Finer morphology was obtained by incorporation of EPDM in PP/HDPE blends and better interfacial adhesion was observed. The EPDM addition increased the percentage of crystallization (χ_c) of PP in PP/HDPE blends.

Panda et al. [59] studied the morphology and dielectric relaxation of ternary blends of PP/PA6/acrylonitrile butadiene styrene copolymer (ABS). It was found that the PP/PA6/ABS (80/10/10) blends exhibited core-shell morphology. A significant reduction in the domain size of the dispersed phase is observed in the presence of PP-g-MAH compatibilizer. The observed shift in α-relaxation peak of PA6 phase is higher in the presence of PP-g-MA as compared to styrene-maleic anhydride copolymer (SMA; with 8% MA content) in PP/PA6/ABS (80/10/10) ternary blends, indicating the higher extent of interfacial reaction between amine end groups of PA6 and maleic anhydride moiety of PP-g-MA.

Lima et al. [60] investigated the effect of ground tire rubber (GTR) and a novel metallocene-based ethylene–propylene copolymer (EPR; with 15 wt% ethylene content) on the morphology and mechanical behavior of ternary polymer blends based on a highly flowable PP homopolymer (MFI of 35 g 10 min^{-1}; 230 °C, 2.16 kg). The incorporation of EPR in the rubber phase of thermoplastic elastomeric blends (TPE) based on GTR and PP (TPE-GTR) has a positive effect on their mechanical performance, attributed to the toughness enhancement of the PP matrix and to the establishment of shell-core morphology between the rubber phases. The mechanical properties of the ternary blends reveal that TPE-GTR blends allow the recycling of this GTR material by injection molding technologies.

This could contribute toward a sustainable approach on the development of TPE-GTR with high processability for the injection molding industry.

Debolt and Robertson [61] investigated the impact strength of ternary blends of PP, polyamide 66 (PA66), and PS. When the ionomer (a copolymer of PE (80%) and poly(methacrylic acid-co-isobutyl acrylate) (20%) neutralized (ca. 70%) with zinc) and block copolymer styrene-ethylene-butylene-styrene (SEBS) were added together to PP/PA66/PS, the impact strength increased nearly as the sum of the impact strengths from PP/PA66/ionomer and PP/PS/SEBS, as if each compatibilized particle acted as an energy-absorbing center.

Ternary iPP/atactic polystyrene (aPS)/SBS blends with iPP/aPS weight ratio of 50/50 exhibit co-continuous morphology. Poly(styrene-butadiene-styrene) (SBS) block copolymer acts as a compatibilizer in iPP/aPS immiscible blends and forms an interfacial layer between iPP matrix and dispersed aPS/SBS particles. The SBS strongly interacts with iPP and aPS and it significantly changes their phase morphologies as well as crystallization process in iPP [62].

Jazani et al. [63] investigated the mechanical and morphological properties for PP/PC/SEBS ternary polymer blends. When maleic anhydride grafted styrene-ethylene-butylene-styrene (SEBS-g-MAH) was incorporated into the blend, the type of morphology changed from core-shell composite particles to a mixed of core-shell composite particles, individual particles and rod-like composite particles. The change in dispersed phase morphology promoted by adding the SEBS-g-MAH has generated a range of PP ternary blends with higher impact strength and modulus compared with PP matrix.

Chand et al. [64] modified PP and PET blend by incorporating ultrahigh molecular weight polyethylene (UHMWPE) ranging from 1 to 5 phr. Addition of 2 and 5 phr UHMWPE improved the wear resistance of PP/PET blends at different loads, which has been explained on the basis of improved bonding as compared with pure PP/PET blend as well as the enhancement in hardness by UHMWPE. The wear mechanism of PP/PET/UHMWPE blend is attributed to microcutting, microplowing, and debris formation.

8.6 Manufacturing of PP Blends

The final properties of PP blends are not merely controlled by the formulation design. The desired properties of PP blends are governed by the processing method as well. This section will highlight a number of techniques to produce PP blends.

8.6.1 Melt Blending

Considerable evidence has been accumulated to demonstrate that type of flow is an important factor on morphology development and final particle size of polymer. In

polymer processing, the elongation flow is more effective than the shear flow. Elongational flow generates exponential stretching, while simple shear flow just gives linear stretching, which results that the dispersed phase droplets of blends are broken more efficiently in elongational flow than in shear flow. Moreover, compared to shear deformation field, elongational deformation field consumes less energy to generate the same deformation of polymer. Some attempts have been performed to generate elongation flow based on converging channels, but most of these elongation flows are local and fixed. Yang et al. [65] designed a non-screw plasticizing processing tool known as the vane extruder (VE), which consists of certain groups of vane plasticizing units and can generate higher stress and dynamic elongation flow. The elongation flow is more effective possibly because the positive displacement-type flow dominates the solid conveying mechanism of VE. The vane extruder is a novel polymer processing equipment with a structure completely different from that of the traditional twin screw extruder. The VE consists of a number of vane plasticizing and conveying units (VPCU), which are shown in Fig. 8.5 [66]. Compared with screw extruder, VE showed better mechanical properties and finer dispersed particles because of the positive displacement-type characteristics of solids conveying. A super-tough PP/SBS blend with enhanced tensile strength and thermal stability was obtained via this reactive compatibilization method using VE.

Qu et al. [67] studied the morphology developemt of PP/PS (70/30) blend in a VE. The result shows that the solid pellets of PP/PS blend are melted quickly in the first five vane plasticizing and conveying units (VPCUs), indicating the strong melting ability and short melting length of the VE. Besides, the blend is elongated in both circumferential and axial direction, and the strong elongational deformation field makes the dispersed phase change from stretched striations to droplets rapidly and mix uniformly finally. The results reveal that the droplet size of dispersed phase in blends prepared by VE is smaller than that prepared by twin-screw extruder, indicating VE has better mixing ability than twin-screw extruder.

Shon et al. [68] made an investigation of the development of phase morphology of an immiscible blend PP/PA6 (75/25) in several different commercial mixing

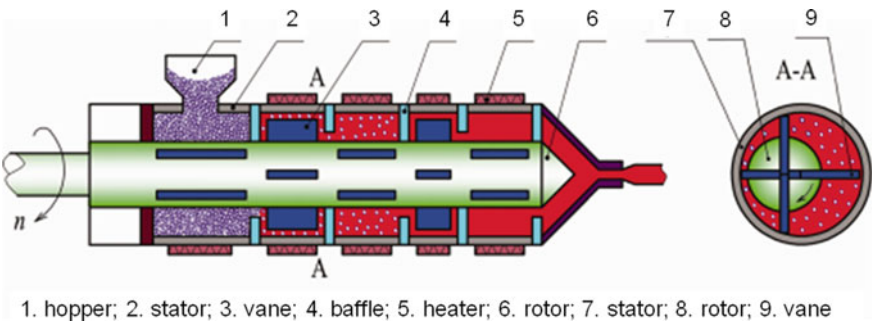

Fig. 8.5 Structural diagram of vane extruder. Adapted from Jia et al. [66], with permission of John Wiley & Sons

machines, i.e. a Buss Kneader, an intermeshing co-rotating twin screw extruder, an intermeshing counter-rotating twin screw extruder, and a continuous mixer. It was found that the intermeshing counter-rotating machine gives the finest dispersed morphologies. According to Polaskova et al. [69] extrusion of immiscible polymers under special conditions can lead to creation of microfibrillar-phase morphology, ensuring significant increase of mechanical properties of polymer profiles.

It has been found that vibration affects diffusion and rate-sensitive processes such as crystallization dynamics and blending. In polymer processing, many prospective vibration technologies such as ultrasonic vibration or mechanical vibration have been used. Wang et al. [70] developed a vibration internal mixer to prepare PP/UHMWPE blends with two additional adjustable processing parameters (vibration frequency and vibration amplitude) as compared with those prepared in the steady mode. Blending PP with UHMWPE, in an oscillatory shear parallelly superposed on a steady shear in the internal mixer, exhibited the different torque vs. time curves possibly embodying energy-saving and higher efficiency compared with blending in the steady shear mode. Vibration can enhance diffusion and dispersion causing different blending effects and forming the corresponding internal structure and better product properties. The forced vibration also increased the interpenetration of two phases. Subsequently, the formed crystals of two components are possibly connected and there is epitaxy of PP and UHMWPE crystals. The larger amount of the small crystals, especially the β-form in the bulk α-form PP together with the co-continuous phase morphology contributes to the higher mechanical properties of PP/UHMWPE.

A reactive extrusion process employing peroxide derived free radicals will significantly affect crystallizable PP chains. Melt-grafted chains have been shown to increase the crystallization temperature of PP. Tortorella and Beatty [71] prepared iPP with an ethylene-octene copolymer using reactive blending. Free radical polymerization of styrene and a multifunctional acrylate during melt extrusion has resulted in the formation of unique features in both amorphous and crystalline phases. Reactive extrusion has significantly altered the size, shape, and distribution of lamellar crystals in PP. It was found that grafting leads to significant changes in the α-crystalline phase of PP and promotes the formation of the β-phase.

Teng et al. [72] prepared compatibilized PP/PA6 blends with PP, ε-caprolactam and PP-g-MAH (MA content 0.5 wt%) via in situ polymerization and in situ compatibilization in a batch mixer. It was found that a PP/PA6 blend containing near uniform distribution of PA6 domain sizes with a mean size of 64 nm can be prepared using the reactive blending method. This very fine dispersion of PA6 component in the continuous PP matrix is expected to provide desirable properties such as thermodynamically stable polymer blends structured on sub-micrometer length scales, improved material transparency, creep and solvent resistance, and favorable rheological properties.

8.6.2 Fiber Spinning (Microfibril and Nanofibril)

Bicomponent fibers offer several advantages over monocomponent fibers. In a core–sheath configuration a bicomponent fiber can display both the surface properties of the sheath material and the mechanical properties of the core material. The two most commonly used materials in carpeting applications are polyamide (PA6 and PA66) and PP. PP carpets are considered to have wear resistant inferior to those of PA. An ideal carpet fiber would combine the best properties of these polymers. Thus, a melt-pigmented PP sheath, PA6 core fiber would be an improvement over conventional monocomponent PA or PP fibers. Godshall et al. [73] produced a bicomponent fiber consisting of iPP sheath and PA6 core that would be suitable for use in a pigmented carpeting application by using fiber spinning technique. In the study of Fallahi et al. [74], blends of PP, PA6 and PP-g-MAH compatibilizer were spun into continuous filaments by an extruder. The fibrils have diameter less than one micrometer. Further, the diameter of the fibrils was decreased by cold drawing. The PA6 matrix can transfer the applied stresses to the fibrils in the longitudinal direction and elongate the PP fibrils during the blend filament drawing.

An electrically conductive or semiconductive network is one of the key aspects of smart and technical textiles. Melt-blending of a common fiber-forming polymer with an intrinsically conductive polymers (ICP) and then melt-spinning the mixture into fibers provides an interesting approach. Soroudi and Skrifvars [75] prepared melt spun drawn fibers using a ternary blend of PP/PA6/PANI (polyaniline) complex. When the ternary blend fibers were compared to the PP/PANI binary fibers, the formers were able to combine better conductivity (of an order of 10^{-3} S cm^{-1}) with a greater tensile strength only at a draw ratio of 5. The results indicated that the draw ratio was a more critical factor for the ternary blend fibers, as both conductivity and tensile strength depended on the formation of fibrils from the core-shell droplets of the PA6/PANI-complex.

8.6.3 Blown Film

Auinger and Stadlbauer [76] investigated the process stability of the blown film from different PP and high melt strength (HMS)-PP blends. Three commercial PP grades were dry-blended with two different HMS-PP grades with varying weight content in the range of 5, 10, and 20 wt%. The maximum stable output could be enhanced up to 50 wt% due to the addition of HMS-PP in accordance to neat PP-grades. The main reason for increasing the output rate is the increase of the strain hardening index (SHI) by the addition of HMS-PP.

8.6.4 Microlayer Co-extrusion

Homogeneous dispersion of a high barrier polymer in a polyolefin matrix does not produce the desired barrier enhancement. Generally, the barrier properties follow those of the continuous matrix. Laminar morphology of the dispersed barrier phase is paramount to achieve good barrier properties. Nanolayer and microlayer coextrusion is a method for combining two or three polymers as hundreds or thousands of alternating layers with individual layers as thin as tens of nanometers. The possibility for utilizing microlayer coextrusion as a tool for creating microplatelets of high aspect ratio was explored by Jarus et al. [77]. PP was combined with PA66 in microlayers, in the presence of PP-g-MAH compatibilizer. A high volume fraction of PA66 microplatelets dispersed in PP was achieved by injection molding the microlayered materials at a temperature intermediate between the melting points of the two constituents. The difference in melting temperatures provided a broad processing window of about 60 °C in which the PP layers melted to form the matrix whereas the PA66 layers remained in the solid state as dispersed microplatelets of high aspect ratio. An enhancement of 4–5 times over the barrier of the conventional melt blend resulted from increased tortuosity of the diffusion pathway. Despite the large difference in melt viscosities, it was possible to combine PP and PA66 as microlayers with more than 2000 layers and nominal layer thicknesses as small as 0.5 μm. Retention of the layered PA66 structure during subsequent injection molding proved this to be a viable route to produce parts containing dispersed microplatelets and nanoplatelets.

8.6.5 Microporous Membranes and Barrier Film Processing

Microporous flat films with possible use as membranes were produced via melt processing and post-extrusion drawing from immiscible PP/PS blends containing a compatibilizing copolymer. The blends were first compounded in a co-rotating twin screw extruder and subsequently extruded through a sheet die to obtain the precursor films. These were uniaxially drawn (up to 500%) with respect to the original dimensions to induce porosity and then post-treated at elevated temperatures to stabilize the resultant structure, which consisted of uniform micro-cracks in the order of a few nanometers in width. Comparison of some of the novel microporous structures of this work with commercial membranes prepared by solvent-based phase inversion processes suggests comparable pore size and porosity ranges, with narrower pore size distribution [78]. The employed melt processing method has several potential advantages over other membrane fabrication processes, especially for solvent-resistant membranes: (1) membrane structure can be tailored by adjusting blend components and/or process parameters, (2) high production rates resulting in lower production cost, and (3) a wide variety of polymer systems having different physical and chemical properties can be used as starting materials.

Polymer membranes are increasingly employed for separation processes. They are relatively economic and cover a broad range of applications from microfiltration to reverse osmosis. Sadeghi et al. [79] investigated a polymer blend of branched and linear PP, to develop microporous membranes through melt extrusion (cast film process) followed by film stretching. Adding a small amount of branched PP into linear PP significantly increased the amount of entanglements in the melt state resulting in strain hardening. The early formation of entanglements during melt stretching created a specific crystalline structure for the blend upon crystallization in the precursor film, which favored orientation of the crystals blocks and also improved the tensile strength in the machine direction. The larger amount of pores and porosity are the result of such structure developed under stretching. The permeability of the samples to water vapor and N_2 was significantly enhanced (more than twice) for the blend system.

Polymer blending by extrusion followed by stretching the extruded film at the exit of the die was found to impart the obtained film with barrier properties. Ethylene vinyl alcohol (EVOH) is usually combined with PP in multilayer structures by co-extrusion process. The effects of different functionalized PP and diethyl maleate (DEM) combined with SEBS on various properties of extruded-stretched films of PP/EVOH blends were studied. Melt blending was done in a co-rotating twin-screw extruder through a flat film die. The stretched films of the original PP/EVOH blends and those of the PP-g-DEM and SEBS-g-DEM modified blends showed lamellar-type morphology, whereas PP-g-MAH and SEBS-g-MAH compatibilized PP/EVOH showed fibrillar morphology. Such peculiar morphology resulted in a dramatic decrease of oxygen permeability as compared with the unmodified or MAH modified PP/EVOH blends. The permeability of PP/EVOH (83.5/16.5) nonstretched film and stretched film (at draw ratio 5) is 61.4 and 20.6 mm $cm^3/(m^2$ day atm), respectively. At draw ratio of 5, the permeability of PP/EVOH/SEBS-g-MAH (81.5/16.5/2) and PP/EVOH/SEBS-g-DEM (81.5/16.5/2) is 32.1 and 0.007 mm $cm^3/(m^2$ day atm), respectively. It was found that shape factor has a slightly more important effect on permeability than interfacial adhesion [80].

Mohanraj et al. [81] reported the solid-state die-drawing of PP and blends of PP with a polyethylene elastomer to produce highly oriented products with enhanced mechanical properties. The blends showed an improvement in the drawability compared to the PP homopolymer. The addition of elastomer modifier particles (i.e., ethylene octane copolymer containing 25% octane) reduced the draw stress significantly, and allowing the blend to be easily oriented at low draw temperatures.

8.6.6 Electron Beam Irradiation

High energy electrons have been used to induce chemical crosslinking in 50/50 blend of PP and NR. The variation of absorbed dose (150–350 kGy) at fixed electron energy (1.5 meV) brings a dramatic change in the properties of the polymer blend. Polyfunctional monomers (PFMs) are used as co-agent during the

electron beam crosslinking of polymers. Dipropylene glycol diacrylate (DPGDA) was added during melt mixing for samples containing the PFM. The use of a PFM resulted in an increased tensile property at a reduced dose level and helped in generating higher graft-linkage at the interface of PP and NR [82].

Modification of polymers and polymer blends in the presence of high-energy irradiation is a potential method for the development of materials with superior properties. Radiation-crosslinked polyolefins are widely used as heat-shrinkable materials because they can store elastic memory that can be recovered upon application of heat. The phenomenon is referred to as memory effect or elastic memory. Polyfunctional monomers, such as multifunctional acrylate, methacrylate, and allylic reactive molecules, blended with the base polymers help achieve crosslinking at a reduced radiation level without a significant deterioration of the base polymers. Ali et al. [83] prepared PP/PE blends in the presence of trimethylol propane trimethacrylate (TMPTMA) monomer. The prepared polymeric samples were cured using an electron beam accelerator at different irradiation doses ranging from 5 to 50 kGy. Incorporation of TMPTMA monomer was found to positively influence the gel content of all samples. The mechanical strength increases on increasing the irradiation dose and attains its highest value at 20 kGy; a more pronounced effect was observed due to incorporation of TMPTMA into iPP than LDPE samples at low irradiation doses.

8.6.7 Foaming

PP foam products are widely used in cosmetics and in the packaging of food and electronics. Therefore, PP foam serves as an alternative to PS foam in the packaging industry. Compared with PS and PE, the foaming process for PP is difficult to control. The poor foamability of PP is because of its high crystallinity and low melt strength. Wang et al. [84] investigated the effect of polydimethylsiloxane (PDMS) on the foaming properties of block-copolymerized polypropylene (B-PP) by blending different contents of PDMS with B-PP in the extrusion process using supercritical CO_2 as the blowing agent. The experimental results indicate that the addition of PDMS greatly increased the expansion ratio of the foamed samples. At the same time, the cell population density of foams obtained from the blends also increased to a certain degree and provided a new perspective on improving B-PP's foaming performance. The maximum expansion ratio of the foam samples obtained from the PP matrix was just seven-fold, whereas the maximum expansion ratio of foams from the PP/PP-g-MAH/PDMS blends with a weight ratio of 98/1/1 was almost 14-fold. This is due to the fact that PDMS has high CO_2 solubility and high CO_2 infiltration capacity.

In general, to produce foam products successfully, PP had to be modified. The crystallinity and melt strength had great effect on the microcellular foamability. The blend with lower crystallinity and higher melt strength had better cellular structure and broader temperature range suited for microcellular foaming. Zhang et al. [85]

prepared PP/PE blends by using microcellular foaming. The relationship between crystallinity, melt strength, and cellular structure was studied. At PE content of 30%, the melt strength and PP melting point were highest and the PP crystallinity was least. The blend with lower PP crystallinity and higher melt strength had better cellular structure and broader microcellular foaming temperature range. It was established that the blend with higher melt strength can be microcellular foamed in a broader range of foaming temperature.

In the study of Spitael and Macosko [86], several PP and their blends were foamed in a continuous twin-screw coextrusion foaming line with carbon dioxide as the blowing agent. Blends of low concentrations of branched polymer in the linear PP show significant strain hardening. Strain hardening is expected to prevent cell coalescence and lead to higher cell concentrations. It was found that even small amounts of branched PP blended in linear PP can improve the foaming process.

8.6.8 Water-Assisted Injection Molding

The obtaining high contents of β-form crystals during processing are of practical importance to enhance the toughness of iPP products. The idea of reinforcing and toughening the iPP via the in situ microfibrillation of a high strength polymeric β-nucleating agent is more attractive and of more practical importance. Wang et al. [87] investigated the phase and crystal morphologies of iPP/acrylonitrile–styrene copolymer (SAN; as β-nucleating agent) blend part molded via water-assisted injection molding (WAIM). Comprehensive analysis of both experimental and simulated results showed that not only the shear flow field but also elongational flow field occurring during the WAIM was responsible for the formation of SAN microfibers and unique crystal morphology distribution in the WAIM iPP/SAN blend part.

8.6.9 Rotational Molding

Polymer blends can address the growing needs of the rotational molding industry by providing new tailored materials with good balances of properties. PP has seen growing interest in rotational molding, because of its high stiffness and good performance at high temperatures. Wang and Kontopoulou [88] had investigated the performance of PP/ultra low density ethylene-α-olefin copolymer (or polyolefin plastomer, POP) blends in rotational molding. The sinter melting curves of these blends exhibited bimodality, due to the wide melting point difference between the two polymers. Increasing POP content resulted in higher sintering and densification rates. Blends of PP with polyolefin plastomers can be rotomolded successfully, yielding products with good ductility and impact properties compared to pure PP. It was also established that using components with lower viscosity results in better sintering and densification characteristics attributed to the enhanced flow properties.

8.6.10 In Situ Polymerization

The versatility of polymerization processes made possible the production of blends in situ directly in the reactor. Blends of iPP, EPR, and ethylene-propylene crystalline copolymer (EPC) can be produced through in situ polymerization processes directly in the reactor and blends with different structure and composition can be obtained. Pires et al. [89] studied the structure of reactor-made blends of PP, EPR, and EPC produced by a Ziegler-Natta catalyst system. For higher ethylene concentration in the feed, rich ethylene rubber was formed, as well as a higher amount of EPC.

8.6.11 Microcellular Injection Molding and Dynamic Packing Injection Molding

Microcellular injection molding is a very effective method to produce excellent dimensional stability parts with lower injection pressure, shorter cycle time, and less material. Polymer blending could provide a new way to prepare microcellular foams with much higher cell density and smaller cell size in microcellular injection molding [90].

The properties of polymer blends depend strongly on processing, for the phase morphology and crystalline structure can be controlled by the stress and temperature field existing in processing. To realize in-process morphology control, generally a prolonged oscillating shear field is imposed on the polymer melt during the packing stage of injection molding, leading to a high orientation of molecular chains and an anisotropic morphology. It is possible to control the phase morphology and crystalline structure of polyolefin blends according to the concept of in-process morphology control by dynamic packing injection molding (DPIM) technique [91].

8.7 Structure-Property Relationship

8.7.1 Impact Modification and Toughening

PP exhibited low fracture toughness at low temperature range under its glass transition temperature. The high notch sensitivity of PP at room temperature often limits its industrial applications. It is known that elastomer-toughened PP blends are one of the strategies to obtain PP with higher toughness. Some of the recommended elastomers and polymers for PP toughening are ethylene-propylene copolymer (EPR), ethylene-propylene diene monomer (EPDM), ethylene vinyl acetate copolymer, styrene-butadiene-styrene (SBS), styrene-ethylene-butadiene-styrene copolymers (SEBS) and poly(ethylene-octene) (POE).

It is well known that toughening in PP/rubber blends is due to crazing and shear yielding of the matrix. The impact modifier particles act as stress concentrators initiating plastic deformation of matrix strands between the rubber particles. Moreover, cavitation inside the particles or at the interface has to be induced as an important precondition for effective toughening. The toughening efficiency depends greatly upon the type of rubber, the loading of rubber, the rubber particle size and distribution, the interparticle distance, and the test conditions [26].

Tang et al. [92] studied the influence of ethylene/styrene interpolymer (ESI) impact modifier on the toughening of PP random copolymer (RC-PP). The ESI have substantially random incorporation of styrene except successive head-to-tail styrene chain insertions. ESI shows excellent compatibility and good toughening effect to styrenic polymers, polyolefins, and a wide variety of other thermoplastics due to their inherent combination of olefinic and styrenic functionality in the backbone of polymer chains. ESI is an effective impact modifier for RC-PP and super-toughened polymer blends are achieved with low amount of ESI (ca. 5 wt%). RC-PP/ESI blends exhibit significant enhancement in toughness and ductility, but shows slightly reduction in tensile strength and elastic modulus with the addition of ESI. SEM observations reveal that the improved impact strength of RC-PP/ESI blends is attributed to cavitation and shear yielding of matrix RC-PP.

Polymer blends of RC-PP and poly(ethylene-octene) (POE) were prepared by melt-blending process using a co-rotating twin-screw extruder. The POE content was varied up to 35 wt%. RC-PP/POE blends exhibited significant enhancement in toughness and ductility. Super-toughened RC-PP/POE blends (Izod impact strength more than 500 J/m) can be readily achieved with only 10 wt% of POE [93].

Poly(ethylene oxide) (PEO) was used as impact modifier to tailor the toughness of iPP. An optimum performance was achieved at a medium PEO content of 15 wt % where the toughness was enhanced by 300%, while the strength only decreased slightly. When the PEO content is less than 15 wt%, it is well dispersed in the iPP matrix, and the addition of PEO also induces moderate amounts of β-form PP. The dispersed PEO could not crystallize and these numerous non-crystallized PEO microspheres are embedded in iPP spherulites, which is mainly responsible for the toughening in the iPP/PEO blends. Nevertheless, when the PEO content is greater than 15 wt%, the PEO phase becomes crystallized and phase segregation takes place, resulting in a drastic deterioration in mechanical properties [94].

Zhang et al. [2] prepared a blend of PP with a toughening master batch (TMB). The TMB were synthesized in a low-viscosity reaction system by using dynamic vulcanization technique starting from PP as matrix resin and ethylene-propylene or butadiene-styrene elastomer as toughening agent through polymer-bridge conjunction derived from a bridging agent monomer containing a carbonate group in the presence of a free radical initiator. In most of the TMB, over half the elastomers existed in a network form, and some of the PP was also connected with elastomers through the polymer bridging or branched chain of bridging agent. The TMB have given the toughened PP similar structural characteristics as with ABS and high

impact polystyrene (HIPS), while an excellent toughness with good rigidity remained.

According to Kakkar and Maiti [95] the impact strength of iPP can be increased by adding 0.32 volume fraction of ethylene vinyl acetate copolymer (EVA). The enhanced impact strength may be attributed to the flexibility effect of EVA, which, along with the amorphous chains, cushions the spherulites of iPP, which enabling the absorption of high impact energy.

Premphet and Paecharoenchai [96] investigated blends of PP and metallocene produced ethylene–octene copolymer (EOR) with a bimodal particle size distribution. The EOR characteristics such as molecular weight (MW), molecular weight distribution (MWD) and octane content showed a strong influence on impact property only when the concentration of EOR in the blends was higher than 10 wt%. High impact strength was achieved by the use of EOR with high octene content and high molecular weight. The critical ligament thickness of approximately 0.3–0.4 μm was observed for the PP/EOR blends. The impact strength increased dramatically with decreasing the ligament thickness below this critical value. Above this critical value, the characteristics of rubber showed no role on toughening efficiency.

The propylene-co-poly(ethylene-propylene) copolymer is one of the polymers that can be used for the rubber toughening of PP. Thanyaprueksanon et al. [97] synthesized polypropylene-block-poly(ethylene-propylene) copolymer (PP-co-EP) by varying the feed condition and changing the feed gas in the batch reactor system using Ziegler–Natta catalysts system at a copolymerization temperature of 10 °C. The copolymer obtained can be used for PP toughening. The differential scanning calorimetry (DSC), dynamic mechanical analysis (DMA), and SEM results indicated that the PP-co-EP included in the amorphous region of PP and the polymer blends have lower glass transition temperature (T_g), and higher toughness than commercial-grade PP within the low temperature range.

The development and commercialization of olefin block copolymer (OBC) offer new opportunities for polyolefin blends and create a need for understanding their effectiveness on polymer toughening. Liu et al. [98] had investigated the miscibility and mechanical properties of iPP/OBC blends (70/30). The OBC domain size decreases with increasing the 1-octene content in the soft segment. The impact strength of the blends is greatly increased with increasing the 1-octene content in the OBC soft segment. It is believed that the enhanced mechanical properties were due to the increase in iPP/OBC interfacial bonding as the OBC soft segments 1-octene content increased, resulting in substantially higher iPP/OBC adhesion and smaller particle size in the iPP matrix.

Elastomer-toughening of PP occurs always at the cost of the decrease of tensile strength and modulus because of the poor strength of elastomer and the poor interfacial interaction between matrix and dispersed phase. It is well known that β-form PP crystallites show higher toughness. Bai et al. [99] blended two different nucleating agents (NA), such as α-form nucleating agent 1,3:2,4-bis (3,4-dimethylbenzylidene) sorbitol (DMDBS) and β-form nucleating agent aryl amides compounds (TMB-5) with PP/POE blends. Once nucleating agent and POE are simultaneously added into PP, PP/POE/NA blends show great improvement of

toughness even at low POE content. The addition of nucleating agent and elastomer into PP simultaneously shows an apparent synergistic toughening effect for PP. It is well known that the main mode of energy absorption during the impact process of elastomer toughened PP is shear yielding of matrix. The easier the shear yielding of the matrix, leads to the better impact toughness of the blends. The great improvement of PP/POE/NA blends toughness is mainly attributed to two combination factors: (1) shear yielding induced by POE particle during impact deformation, and (2) the effects of nucleating agent which cause the significant decrease of PP spherulites size and the homogeneous dispersion of the spherulites.

In the study of Fanegas et al. [100], iPP blends were prepared with two different thermoplastic elastomers, SEBS and a metallocenic ethylene-octene copolymer (EO). The addition of a nucleating agent (methylene-bis (4,6-di-tert-butylphenyl) phosphate sodium salt) as a third component exerted a significant effect on the overall properties. The improvement of impact properties found in binary blends was accompanied by a decrease in stiffness. However, the addition of the nucleating agent provided a good balance between impact strength and stiffness, which is due to the fact that the nucleating agent generates smaller spherulites, thus improving the mechanical properties.

Grein and Gahleitner [101] studied the effects of nucleation on the toughness of iPP/ethylene-propylene rubber (EPR) blends with different rubber molecular architectures. Two reactor-made iPP/EPR blends were produced with a high yield 4th generation Ziegler-Natta-catalyst. Both grades contained 32 wt% of xylene cold soluble (XCS, approximated to be the EPR content), had a propylene-rich rubber (C3-XCS of about 55 wt%). The rubbery phase of PP-1.9 had an intrinsic viscosity (IV) of 1.9 dl/g, while the dispersed phase of its counterpart, PP-4.2 had an IV of 4.2 dl/g. Figure 8.6 shows that the particle size of the iPP/EPR blends is dependent of the intrinsic viscosity of their elastomer phase. The PP-1.9 exhibited smaller EPR inclusions than its homologue which had an IV of 4.2. Consequently, the inter-particle distance (ID) of PP-1.9 was smaller to than that of PP-4.2. For blends exhibiting a small inter-particular distance between their EPR phases, toughness was promoted slightly by α-nucleation and to a large extent by β-nucleation as compared to the non-nucleated blends. These findings indicate the significance of relationship between the rubbery phase and the matrix to maximize the fracture resistance of polymer blends.

It is known that brittle-ductile transition behaviors of PP/elastomer blends do not only depend on the dispersed elastomer phase, but also on the matrix properties such as crystalline structure and morphology. The presence of large amounts of β-form crystals in the PP matrix is favorable to the shift of brittle-ductile transition towards lower temperatures. Therefore, a notable decrease in brittle-ductile transition temperature of PP random copolymer matrix with soft rubber phase will be expected if extensive β-form crystals could be formed in the matrix [1]. Adding both impact polypropylene copolymer (IPC) and β-nucleating agent (a rare earth agent composed of hetero-nuclear dimetal complexes of lanthanum and calcium containing some specific ligands) into PP random copolymer has three effects: (1) leading to a significant enhancement in β-crystallization capability of PP

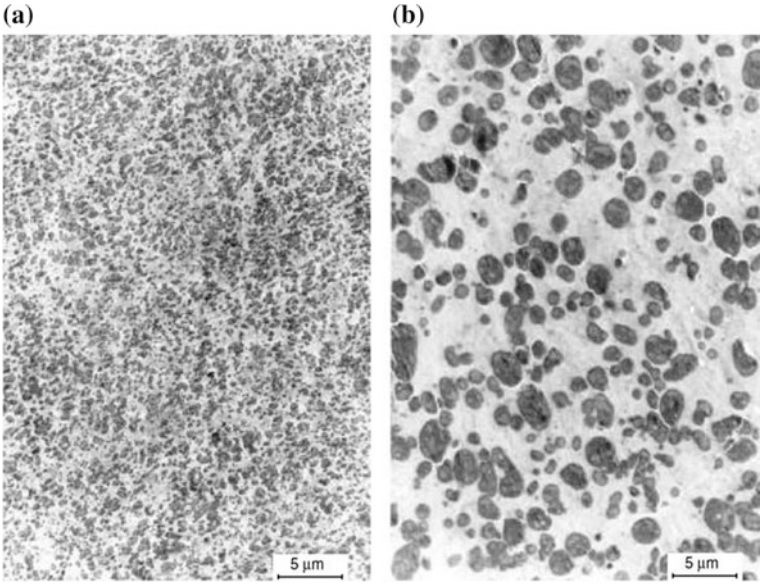

Fig. 8.6 Transmission electron micrograph of ruthenium tetroxide (RuO4) stained PP-1.9 and PP-4.2. Adapted from Grein and Gahleitner [101], with the permission of BME-PT

random copolymer, (2) contributing to the shift of brittle-ductile transition to lower temperatures, (3) increasing the brittle-ductile transition rate. The reason for these changes can be explained by two phenomenons. First, the transition of crystalline structure from α-form to β-form reduces the plastic resistance of PP random copolymer matrix, thus facilitates the initiation of matrix shear yielding during the impact process. Second, the well dispersed rubbery phase in IPC with high molecular mobility at relatively low temperatures is beneficial to the shear yielding of PP random copolymer matrix and thus greater improvement in impact toughness of the ternary blends can be achieved [1].

Jafari and Gupta [102] used two elastomers (EVA and EPDM) as impact modifier for PP. EPDM is found to be a better impact modifier for PP by increasing the impact strength of PP by a factor of up to about 20, whereas the EVA showed only two times the improvement in impact properties of PP. The analysis of dynamic mechanical properties revealed that there is a direct correlation between impact strength and loss peak area, that is, the impact strength of blend increased with the increase of the loss factor. This suggested that the energy of dissipation due to viscoelasticity of the blend is an important mechanism of impact toughening of PP/EVA blend. The energy dissipation due to viscoelastic relaxation is therefore suggested as a mechanism of impact toughening of PP, in addition to the other commonly known mechanisms of toughening (i.e., shear yielding and crazing induced by deformation of rubber-phase domains). Thus, in addition to commonly

known mechanisms of impact toughening, the energy dissipation due to viscoelasticity should be taken into account for designing supertough PP.

8.7.2 Crystallization

The high tendency of iPP to crystallization is due to its regular chain structure. A similar tendency to crystallization is implied in propylene copolymers with relatively low comonomer content (ethylene, olefins), e.g. block copolymers (BC-PP) and random copolymers (RC-PP) [103]. The β-nucleated iPP homopolymers have received considerable interest recently. This interest is mostly due to the peculiar thermal and mechanical performance of the β-crystalline PP [104]. It was well known that β-PP possessed higher toughness and heat distortion temperature than those of α-PP. If β-PP blends with other polymers could be prepared, they could be obtained with higher toughness and heat distortion temperature. In this section, the research findings on how to increase the β-PP content as well as crystallization rate of PP are documented. On the other hand, it is also important to know some of the opposite findings, e.g., inappropiate usage of compatibilizer/additives, inappropriate cooling rate and processing condition (mold temperature, injection speed) can reduce crystallization rate and/or suppress the β-PP nucleation.

It was found that addition of other crystalline polymers gives different effects on the β-nucleation of PP blends. The β-nucleation of PP in the blends depended on the preparation methods and the crystallization temperature and α-nucleation of other crystalline polymers. If the crystallization temperature of other crystalline polymers was lower than that of PP or the α-nucleation of the second component was weak, the second component would not affect the β-nucleation of PP in the blends, e.g. with LDPE. On the other hand, if the crystallization temperature of other crystalline polymers was higher than that of PP, the α-nucleation of the second component could markedly decrease the β-nucleation of PP in the blends, and it was difficult to prepare β-PP blends with high content of β-crystal [15].

According to Zhang and Robert Kwok [5] β-PP can be detected only when the PA6 content is lower than 3 wt%, which indicates that PA6 strongly suppresses the formation of β-PP. Thus, the preparation of PP/PA6 blends with β-PP matrix is very difficult. The reason is that the β-nucleating agent is selectively encapsulated in the polar phase. However, suitable compatibilizers can assist the distribution of the β-nucleating agent between both phases of the blend and promote the formation of a matrix rich in β-PP. It was found that higher β-PP content could be obtained by adding the β-nucleating agent to the PP blends at a temperature below 190 °C.

Zhang et al. [15] prepared β-PP/PS blends with PP, PS, and a novel supported β-nucleating agent or β-nucleated PP and PS. The results indicated that the PP with high content of β-crystal was obtained by addition of calcium carbonate ($CaCO_3$) supported β-nucleating agent into PP. Nevertheless, the addition of compatiblizers, e.g. PP-g-MA, glycidyl methacrylate-grafted PP (PP-g-GMA), and maleic

anhydride-grafted ethylene vinyl acetate copolymer (EVA-g-MA) slightly decreases the β-nucleation of PP in these blends.

Wang et al. [105] studied the morphology development during isothermal crystallization in equal molecular weight iPP and atactic polypropylene (aPP) blends with time-resolved simultaneous small-angle X-ray scattering (SAXS) and wide-angle X-ray scattering methods with synchrotron radiation. A detailed analysis of the SAXS patterns indicates that aPP disrupts the ordering within the lamellar stacking. The results are generally consistent with predominantly interfibrillar incorporation of the aPP diluent within the microstructure, with only modest interlamellar incorporation dependent on the crystallization temperature.

Finlay et al. [106] studied the properties of slowly cooled iPP/HDPE blends. At slow cooling rates, the HDPE and iPP components in the blends crystallize at lower temperatures than in the pure homopolymers, suggesting that the presence of one component inhibits rather than promotes the crystallization of the other.

Borysiak [107] found that incorporation of poly(styrene-ethylene-butylene-styrene) grafted with maleic anhydride (SEBS-g-MA) block copolymers into iPP/PS blends resulted in a significant decrease in β-content of iPP. It was also found that at a higher temperature mold and lower injection speed, the amount of β-phase of iPP matrix slightly reduced.

Yang and White [108] prepared PP mixed with ethylene butene copolymers (EBM; containing 51.6 mol% butane). The EBM could largely decrease the crystallization rates of the PP phase because the EBM molecules diluted the PP molecule concentration, and thus decreased both the nucleation and crystallization growth rates.

Zhang et al. [109] prepared PP/PS blends modified with reactive monomers, such as maleic anhydride (MAH) and styrene (St), and in situ formed PP/PS blends by melting extrusion. The results indicated that the addition of MAH hardly influenced the crystallization temperature of PP in the blends. However, the addition of MAH and St increased the crystallization temperature of PP in its blends, and made PP form a single peak of melting instead of a shoulder peak of melting. This could be attributed to the heterogeneous nucleation of PP-g-MAH, which was in situ formed in melt mixing.

Yang et al. [110] used a highly efficient nano-$CaCO_3$-supported β-nucleating agent to obtain iPP/PA6 blends with a high β-iPP content. PP-g-MA, PP-g-GMA, maleic anhydride grafted poly(ethylene octene) (POE-g-MA), and EVA-g-MA elastomers were added to the blends as compatibilizers. PP-g-MA, POE-g-MA, and EVA-g-MA reduced crystallization temperature of iPP and increased the β-iPP content in the β-nucleated iPP/PA6 blends, and this can be attributed to the fact that the compatibilizer improved the dispersion of PA6 in the iPP phase, resulting in a decrease in the crystalline ability and α-nucleating ability of PA6.

The isothermal crystallization kinetics of blends of different PP resins and a liquid crystalline polymer (LCP) after two different melting conditions (200 and 290 °C) were studied by DSC and polarized light optical microscopy. The resins were a homopolymer (hPP), a random copolymer with 3% ethylene (cPP), and a

grafted copolymer with 0.15% of maleic anhydride (gPP). The LCP was Vectra A950, a random copolymer made of 75 mol% of 4-hydroxybenzoic acid and 25 mol% of 2-hydroxy,6-naphthoic acid. It was observed that the overall crystallization rates of all the blends after melting at 200 °C were higher than those after melting at 290 °C. The LCP acted as a nucleating agent for all the PP resins; however, its nucleating effect was stronger for the hPP than for the cPP and gPP resins. All the PP resins formed transcrystallites on the surface of LCP domains [111]. According to Yu et al. [18] isothermal crystallization showed decreased crystallization half-times with the incorporation of LCP, and these were further reduced with compatibilizer (i.e., PP grafted with epoxy via glycidyl methacrylate). It was again proved that the LCP can act as nucleating agent for PP.

Guan et al. [112] investigated the crystallization behaviors of PP homopolymer and its blends with 0–15% functionalized polypropylene (FPP), the backbones of which were grafted with guanidine and diamide polymer chains. There was about 10 wt% of a modifying agent (guanidine and diamide polymers) grafted onto the backbone of PP in FPP. The FPP increased the crystallization rate. The half-time of crystallization for PP/FPP blends was much shorter than that for the PP homopolymer. FPP acts as a nucleation agent and accelerates the crystallization. The crystallization temperature of PP/FPP blends is 10 °C higher than that of PP. However, blending with FPP does not alter the crystal conformation α-phase monoclinic structure.

Wu et al. [113] investigated the crystallization behavior and morphology of nonreactive and reactive melt-mixed blends of PP and polyamide 12 (PA12). It was found that the crystallization behavior and the size of the PA12 particles were dependent on the content of the PP-g-MAH compatibilizer because an in situ reaction occurred between the maleic anhydride groups of the compatibilizer and the amide end groups of PA12. The compatibilized blends showed fractionated crystallization, which depended on compatibilizer content. An increasing amount of compatibilizer caused a large decrease in enthalpy that was associated with the crystallization of PA12, which completely disappeared when the concentration of compatibilizer was more than 4%. These finely dispersed PA12 particles crystallized coincidently with the PP phase. The in situ formed graft copolymer (PP-MA)–g–PA12 played a role in concurrent crystallization by reducing interfacial tension and increasing the dispersion of PA12.

Random ethylene–propylene copolymer (PP-R) produced by copolymerization of propylene and ethylene is a product of modified PP that has received a great deal of attention in academic and plastic industry. Wang and Gao [114] studied the nonisothermal crystallization behavior and morphology of blends of PP with PP-R. The single peak during the melting and crystallization process indicated that PP and PP-R were very miscible and they are co-crystallizable. The values of the Avrami exponent indicated that the crystallization nucleation of the blends was heterogeneous while the growth of the spherulites was tridimensional. The addition of a minor PP-R phase favored an increase in the overall crystallization rate of PP.

Lin et al. [115] prepared β-nucleated PP, uncompatibilized β-nucleated PP/poly (trimethylene terephthalate) (PTT), β-nucleated PP/PTT blends compatibilized with PP-g-MAH and styrene–ethylene–propylene copolymer. The β-nucleating agent (N,N'-dicyclohexylterephthalamide) was mixed and blended with PP by a twin-screw extruder at temperatures of 170–200 °C to prepare the β-nucleated PP. All of the β-nucleated PP/PTT blends contained β-crystals of PP, and the compatibilizers exhibited synergistic effects with the β-nucleating agent to further increase the content of β-crystals.

Another interesting topic worth to mentioning is the β-transcrystallinity of iPP reinforced by fibers. According to Hao et al. [116] the polyethylene terephthalate (PET) fiber containing higher content of β-nucleating agent (β-NA) has dual nucleation ability, which it has both β- and α-nucleating ability. The β-NA loaded in the PET fiber would lead to dense β-nuclei and enhance the growth of β-transcrystallinity, while the local surface without β-NA of the fiber induce the formation of α-crystallites. The interfacial morphology evolution of iPP reinforced by PET fiber loaded with β-NA and that after being selective melting is schematically shown in Fig. 8.7.

Lima et al. [117] analyzed the effect of ground tyre rubber (GTR), EPDM and EPR on the crystallization of binary and ternary PP blends. Results reveal that GTR has a strong nucleating effect on PP and that its presence leads to higher crystallization rates. The EPDM presence has a slight effect on the PP crystallization

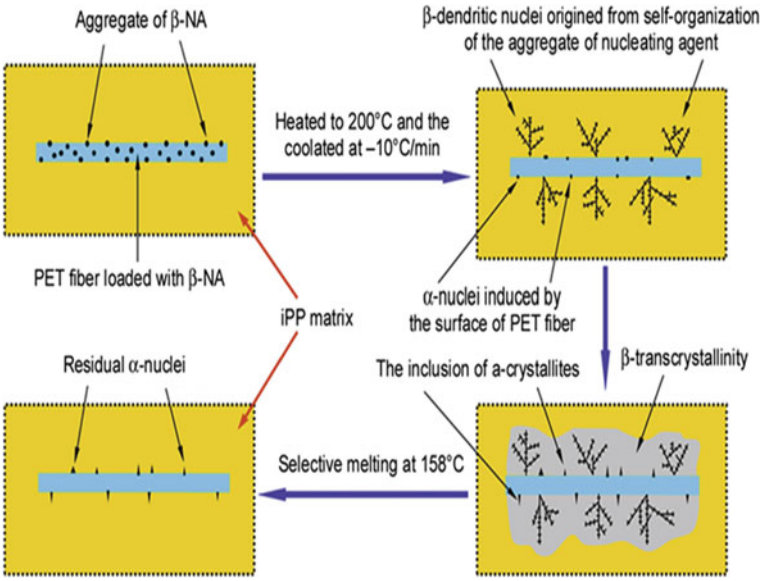

Fig. 8.7 Schematic illustration of the interfacial morphology evolution of iPP reinforced by PET fiber loaded with β-NA and that after being selective melting. Adapted from Hao et al. [116], with the permission of BME-PT

process whereas EPR has no significant effect. A decrease of the half time of crystallization and increase on the rate constant k indicate a significant increase of the overall crystallization rate. The Avrami exponent n values (~ 3) confirm the heterogeneous mechanism and indicate a three-dimensional spherulitic growth.

8.7.3 Rheology

Rheological study of PP blends is an important tool to understand their processability, melt strength, linear viscoelastic behavior, miscibility of the blends component in the melt state, relaxation process as well as phase morphology.

Blends of PP copolymer and a polyolefinic elastomer (POE) were prepared by a melt-blending process at 210 °C and 60 rpm using a counter-rotating twin-screw extruder. The POE content was varied up to 25 wt%. All blend compositions showed well-defined zero shear viscosity and shear thinning behavior. Rheology of PP copolymer/POE blends shows different behavior up to concentrations of POE corresponding to the tough–brittle transition. The linear viscoelastic properties were used to check the miscibility of the two components in the melt state. All blend compositions showed a good degree of miscibility over the range of POE concentrations studied. The PP copolymer/POE system appears to be a miscible blend, at least up to 25 wt% concentration of POE [118].

One of the effective approaches to enhance the melt strength of PP is to add polymers with long chain branches such as ethylene-butene copolymers (PEB). Zhang et al. [119] studied the extensional rheological behavior of PP, PEB and their blends in the melt state. The PEB enhances the strain hardening of the PP. The transient elongational viscosity of the PP/PEB blends with 20 and 40 wt% PEB deviates from the linear viscoelastic envelope at all strain portions, attributed to their morphology evolution during elongation.

It is well known that the representation of the dynamic shear data in Cole–Cole plots (η'' versus η') gives information about the relaxation processes occurring in a multiphase system. This type of representations can also be used to predict the compatibility of polymer blends. It is assumed that when a blend is compatible, a single curve is obtained in this type of plots, independent of the composition of the blend. According to López Manchado et al. [120] plots of η'' versus η' (Cole–Cole plots) show that the PP/EPDM blend with the lower EPDM rubber content (25 wt %) has a certain rheological compatibility with neat PP. A general processing behavior similar to that of PP was observed for blends with low content of EPDM (25 wt%), indicating that the same industrial thermoplastic molding processes used for neat PP can be adopted with evident economic advantages.

Ardakani et al. [121] studied the rheology, morphology and interfacial interaction of PP/polybutene-1 (PB-1) blends. A droplet-matrix morphology was observed for all blends in SEM images. At low concentrations, up to 10 wt% PB-1, the particles size is smaller than 40 nm and homogenously dispersed in the matrix. By increasing the percentage of PB-1 a non-homogenous morphology is obtained and

the size of the droplets increased. The complex viscosity of samples at various percentages of PB-1 showed the log-additivity mixing rule behavior in low frequencies and positive-negative deviation behavior at high shear rates. The phenomena such as decrease in the sensitivity of storage modulus to shear rate in the terminal region, the deviation of Cole–Cole plots from the semi-circular shape, and the tail in relaxation spectrums at high relaxation times are the evidences of two phase heterogenous morphology.

Marguerat et al. [122] investigated the relation of morphology to the linear viscoelastic properties PP/EVA and PP/ethylene methyl acrylate (EMA) blends. The rheological properties of the elastomeric phase were modified by crosslinking in presence of an organometallic catalyst. The Palierne model was used to describe the linear viscoelastic behavior of the blends, and to estimate the interfacial tension between the immiscible components. In general, the Palierne model is used to describe the viscoelastic behavior of blends, assuming a monodisperse distribution in size of the inclusions. It was proved that the Palierne model describes relatively well the linear viscoelastic properties of reactive and nonreactive PP/EVA and PP/EMA blends containing 20 wt% or less elastomer.

Shi et al. [123] studied the melt rheological properties of binary uncompatibilized PP/PA6 blends and ternary blends compatibilized with PP-g-MAH using a capillary rheometer. The experimental shear viscosities of the blends were compared with those calculated from Utracki's relation. The value δ represents the difference between the experimental viscosity, log η, and the calculated one, log η'. The deformation recovery and/or break-up ability of the dispersed droplets greatly affect the final apparent shear viscosity of blends during capillary flow. From the macroscopic point of view, the deviation value δ between the experimental and the theoretical apparent shear viscosity values calculated from Utracki's relation proved to be useful in characterizing the deformation recovery and/or breakup ability of the dispersed droplets in polymer blends. In binary PP/PA6 blends, when the deformation recovery of dispersed droplets plays the dominant role, δ is negative. The higher the dispersed phase content, the more deformed the droplets are and the lower the apparent shear viscosity. Also, the absolute value of δ increased with dispersed phase composition. In ternary PP/PA6/PP-g-MAH blends, when the elongation and break-up of the dispersed droplets play the dominant role, a positive deviation can be found between the experimental and the calculated results. The higher the content of the dispersed phase, the higher the absolute δ values of the ternary blends are and the stronger the positive deviation.

The dynamic rheological behavior is measured by small amplitude oscillatory shear on rotational rheometer for PP/PA6 blends compatibilized by PP-g-MAH. The dynamic rheological measurement shows that when the weight ratio of PP/PP-g-MAH/PA6 increases from 100/6/0 to 100/6/60, the complex viscosity and dynamic modulus at low frequency increase gradually, but when the weight ratio of PP/PP-g-MAH/PA6 continues to increase to 100/6/80 and 100/6/100, the complex viscosity and dynamic modulus decrease. Bousmina's model can fit the data well when the weight ratio of PP/PP-g-MAH/PA6 is 100/6/20 and 100/6/40, respectively. Note that Bousmina's model considers the blend as a three-region system,

that is, spherical droplets surrounded by matrix shells dispersed in a homogeneous matrix. In addition, Bousmina's model considers the flow circulation inside and outside the droplet, hence it can corroborate the experimental data of compatibilized blends [124].

8.7.4 Other Properties

Efforts have been done to solve the limitation or to improve the potential properties of PP, for example, foamability, dyeability and weatherability—in order to widen the applications of PP blends.

8.7.4.1 Foamability

PP has been considered as a substitute for other thermoplastic foam materials. However, some studies have shown that it is not easy to foam PP for three reasons: (1) PP is a semi-crystalline polymer and gases are difficult to dissolve in the crystalline regions, (2) the melt strength of PP is low that the cell walls may not have enough strength to bear the extensional force and may collapse easily during foaming, and (3) the viscosity of PP is dependent on the foaming temperature, that is, even small overheating of the polymer melt leads to a very large drop in viscosity and hence cause the coalescence of bubbles. Thus, the operating temperature interval for PP foaming is quite narrow. Li et al. [125] used polypropylene block (PP-B) copolymer as a modifier to improve the crystallization behaviors and foaming performance of PP homopolymer (HPP). The experimental results indicate that the crystallization temperature and rate of PP-B are higher than those of HPP, so it can be used as the nucleation modifier to improve the HPP/PP-B crystallization behaviors. The higher crystal density and melt strength are advantageous for the improvement of cell structure of the foamed materials. In comparison with pure HPP, the blending of PP-B can make the crystal grain fine dramatically. SEM results show that much more uniform, smaller cells can be obtained for the HPP/PP-B blends. The crystal nuclei formed earlier can act as physical crosslink points, increasing the melt strength and improving dramatically the cell structure and morphology of the HPP/PP-B blends.

Another way to improve the foaming of a linear PP is to incorporate long-chain branches (LCBs). The PPs with LCBs have a pronounced strain hardening, which is closely related to an enhancement of the melt strength. Different methods have been applied to modify PP by LCB. Most of the LCB PP are produced by in situ polymerization and by post-reactor treatment. After the reactor treatment, the LCBs can be formed by reactive extrusion or by electron beam irradiation. Several studies have shown that foaming of LCB PP, either pure branched PP or blended with linear PP, leads to higher expansion ratio and more homogeneous cellular structures. The blends rich in LCB PP show better foamability owing to their higher melt

strength. The balance between the large nucleation of the linear PP and the reduction of the cell coalescence due to the important strain hardening of the LCB PP can lead to a higher cell concentration in the blends of linear and branched PPs than in the neat polymers. While the linear PP does not exhibit strain hardening, the blends of the linear and the HMS PP show pronounced strain hardening, increasing with the concentration of HMS PP. The results demonstrate the importance of the extensional rheological behavior of the base polymers for a better understanding and steering of the cellular structure and properties of the cellular materials [126].

8.7.4.2 Dyeability

As a textile fiber, PP is incapable of being dyed by conventional dyestuffs from an aqueous dye bath because of its nonpolar and highly crystalline structure. These inherent attributes limit the dye receptivity of PP, and this is considered to be the drawback of PP usage in the textile industry. It has been observed that melt blending of PP with PS, PA and polyesters before spinning is an efficient process for enhancing the dyeability of PP fibers. Mirjalili et al. [127] attempted to predict the optimal disperse dye uptake of PP modified with PET and PP-g-MAH compatibilizer without adversely impairing its mechanical properties. For this purpose, the amounts of three independent variables in the blend composition, namely, the weight fractions of PP, PET, and PP-g-MAH, were varied according to a special cubic mixture experimental design. By use of a special cubic experimental design, it was demonstrated that the desired dyeability was attained by the addition of limited amounts (10–15 wt%) of PET. The results indicated that the PP/PET/PP-g-MA blends in which the PET and PP-g-MA contents were in the range 10–15 and 4–5 wt%, respectively, gave maximal dye uptake and desirable tensile properties. On the basis of these results, it was concluded that an optimum PET:PP-g-MAH ratio of 3:1 provided a PP/PET/PP-g-MAH blend with desired dyeability and acceptable mechanical properties.

8.7.4.3 Weatherability

The study of degradation and stabilization of polymers is extremely important from the scientific and industrial point of view, to ensure a long service life of the product. Mouffok and Kaci [128] investigated the degradation of uncompatibilized and compatibilized PP/PA-6 (70/30 wt%) with PP-g-MAH (2 wt%) under accelerated UV light. Fourier transform infrared spectroscopy (FTIR) analysis of the structure of the compatibilized and uncompatibilized blends after exposure to UV light showed the formation of photoproducts corresponding to both components. The overall results suggest that the photooxidation in PP/PA-6 blends starts in PA-6 phase initiating chain oxidation of PP. The photooxidation of the two phases occurs simultaneously due to the interactions between the photoproducts of both

components, increasing the degradation rate of the blend. The compatibilizer acts as a photooxidation promoter in PP/PA-6 blends. Accordingly, to improve the durability of these blends, it is necessary to prevent them against UV degradation by optimizing the quantity and quality of UV stabilizer to be used. In addition, the selection of appropriate compatibilizer for PP/PA6 blends that is more durable in the UV environment should be considered.

8.8 Compatibilization of PP Blends

Most of polymers are immiscible with each other because of the positive Gibbs energy of mixing, which results in phase separation, poor adhesion in interfaces, and deteriorated ultimate properties. Therefore, compatibilization of the immiscible polymer pairs must be taken into full consideration during the design of high-performance polymer blends. Compatibilization of multiphase polymer systems has been reviewed extensively in literature. It is well established that compatibilization can be achieved either by addition of pre-synthesised copolymer (physical compatibilization) or through the in situ generation of graft or block copolymers at the interface between the individual polymers by chemical reactions during processing (reactive compatibilization) [129]. To improve the compatibility of PP blends, suitable compatibilizing agents are often added to the blends to decrease the interfacial tension and achieve more homogeneous dispersion with smaller domain size. Reactive compatibilization is another interesting method from economic and academic points of view in which the compatibilizer is generated during the blending process and preferentially locates at the interface.

8.8.1 Physical Compatibilization

Styrene-butadiene-styrene (SBS), styrene-ethylene-butadiene-styrene (SEBS), styrene-ethylene-propylene (SEP), styrene-isoprene-styrene (SIS), and polypropylene-g-polystyrene copolymer (PP-g-PS) are some of the recommended compatibilizers for PP/PS blends. Among which, PP-g-PS graft copolymer, composed of a PP backbone and PS branches, is an ideal compatibilizer for PP/PS blends due to the good compatibility of PP backbone and PS branches with PP bulk and PS bulk, respectively. Wang et al. [130] evaluated the effects of PP-g-PS on the morphological and rheological properties of PP/PS blends. The results revealed that the addition of PP-g-PS graft copolymers significantly reduced the PS particle size and enhanced the interfacial adhesion between PP and PS phases. According to Li et al. [131] DMA and SEM results illustrated that the PP-g-PS is an efficient compatibilizer for the PP/PS blend. The phase separation decreased when PP-g-PS was added. This phenomenon is much clearer when the PP/PS blend ratio is 75/25.

The presence of PP-g-MAH increases the phase stability of PP/PS (90/10 and 80/20) blends by preventing the coalescence. Hence, finer and more uniform droplets of PS dispersed phases are observed. The compatibilizer induced some improvement in impact strength for the blends. The degree of crystallinity of PP/PS (80/20) blends was increased from 38.8 to 49.2% by the addition of 10 wt% PP-g-MAH [132]. According to Slouf et al. [133] styrene-ethylene-propylene (SEP) can act as an efficient compatibilizer of iPP/atactic PS blends.

Syed Mustafa et al. [134] investigated the use of an aromatic vinyl monomer (AVM)-grafted PP (PPA) as a compatibilizer for PP/PS blend. PPA was prepared by grafting a monofunctional aromatic vinyl monomer onto PP using organic peroxide at 180 °C for 10 min in a Brabender mixer. Results obtained from tensile and impact strength, heat deflection and melt flow index measurements show some improvement in the properties of the blends indicating some compatibilization effects in the blend system.

Mandal and Chakraborty [135] prepared PP blends with thermotropic Vectra B-950 liquid crystalline polymer (LCP; an aromatic copolyesteramide comprising 60 mol%, hydroxy naphthoic acid, 20 mol%, terephthalic acid, and 20 mol% p-aminophenol) in different proportions in presence of 2 wt% of ethylene-acrylic acid copolymer (based on PP) as a compatibilizer. The tensile properties of the compatibilized blends displayed improvements in modulus and ultimate tensile strength of PP matrix with the incorporation of 2–10 wt% of LCP incorporation. The development of fine fibrillar morphology in the compatibilized PP/LCP blends had large influence on the mechanical properties.

Mandal et al. [136] prepared blends of PP and Vectra A950, a thermotropic liquid crystalline polymer (LCP; an aromatic copolyester comprising 25 mol% of 2,6-hydroxynaphthoic acid and 75 mol% of para hydroxybenzoic acid) blends were prepared in a single-screw extruder with the variation in Vectra A950 content in presence of fixed amount (2 wt%, with respect to PP and LCP mixture as a whole) of ethylene-acrylic acid (EAA) copolymer as a compatibilizer. Mechanical analysis of the compatibilized blends within the range of LCP incorporations (2–10 wt%) indicated pronounced improvement in the modulus, ultimate tensile strength and hardness. FTIR results confirmed the existence of strong interaction between the segments of EAA and LCP Vectra A 950 through intermolecular H-bonding in the blends. This investigation demonstrates that the preferential alignment (fibrillar morphology) of Vectra A950 during melt blending as well as the enhanced interfacial adhesion between Vectra A950 and the compatibilizer EAA play the key role in improving the mechanical properties of the blends.

The grafting polymer containing maleic anhydride (e.g. PP-g-MAH) or epoxy glycidyl methacrylate (e.g. PP-g-GMA) groups can potentially react or become involved in hydrogen bonding with hydroxy or carboxy on the LCP polyester and provide compatibilization between the phases. Liquid crystalline polyester was dispersed in PP to provide a coarse two-phase incompatible blend. Glycidyl methacrylate grafted polypropylene was effective as a compatibilizer, and smaller particles of LCP were formed with good interfacial adhesion [18].

Farasogldu et al. [137] used PP-g-MAH to compatibilize PP/LCP blends. Two types of LCP were used, namely Vectra A950 (VA; based on 73% hydroxybenzoic acid and 27% hydroxynapthoic acid) and Vectra B950 (VB; synthesized from 60% hydroqnapthoic acid, 20% terepthalic acid and 20% aminophenol). It was found that the greater enhancement in tensile modulus, yield stress, yield strain and thermomechanical behavior is obtained for 5% compatibilizer content in either 10 or 20% per weight LCP phase.

Lee et al. [138] investigated the effects of SEBS-g-MAH on the mechanical and morphological properties of PP/ABS blends. The PP/ABS (70/30) blends containing SEBS-g-MAH showed improved impact strength with minimal tensile strength loss. This result suggests that MAH in SEBS-g-MAH plays an important role as an impact modifier and compatibilizer with the PP/ABS blend, possibly because of dipolar interactions between the MAH group and polar group in ABS.

The polypropylene-graft-cardanol (PP-g-cardanol) was prepared by reactive extrusion with PP and natural renewable cardanol which could increase the interfacial energy of PP and inhibit the degradation of PP during the process of reactive extrusion and usage. Cardanol grafted onto PP could inhibit the light and heat degradation because the natural product of cardanol had the dual effect of electron donating and electron withdrawing due to the p–π conjugated system of cardanol. PP-g-cardanol and PP-g-MAH were used as compatibilizers of the PP/ABS blends. From the results of morphological studies, the droplet size of ABS was minimized to 1.93 and 2.01 μm when the content of PP-g-cardanol and PP-g-MAH up to 5 and 7 phr, respectively. The results of mechanical testing showed that the tensile strength, impact strength and flexural strength of PP/ABS (70/30) blends increase with the increasing of PP-g-cardanol content up to 5 phr [139].

Lee and Kim [140] examined the effect of three compatibilizers, i.e. a hybrid compatibilizer composed of PP-g-MAH and polyethylene-glycidyl methacrylate (PE-g-GMA), a single PP-g-MAH compatibilizer, and a single PE-g-GMA compatibilizer on the mechanical, morphological, and rheological properties of a ternary blend of PP, poly(lactic acid) (PLA), and a toughening modifier (Biomax Strong 120). The tensile strength, flexural strength, and impact strength of the ternary blends (PP/PLA/toughening modifier: 60/30/10) with a hybrid compatibilizer content of 3 phr exhibited better material properties than the blend containing only a single compatibilizer.

Dai and Ye [141] investigated a series of compatibilizers, including polypropylene (PP) grafted with 2-tertbutyl-6-(3-tertbutyl-2-hydroxy-5-methylbenzyl)-4-methylphenyl acrylic ester (BPA), glycidyl methacrylate (GMA), GMA/styrene (GMA-st), and 2-allyl bisphenol A for the purpose of improving the compatibility of PP/PC blends. PP-g-BPA shows a remarkable compatibilizing effect on PP/PC blends since it has similar group—benzene ring with PC, and it is a sort of heat-resistant antioxidant in the meantime, which can reduce the molecular degradation of PP during grafting and blending under high temperatures. The blending morphologies change from the cylinder-shaped domains to a spherical shape and more reduced homogeneous size of the dispersed PC particles by addition of PP-g-BPA.

Zhang et al. [142] prepared ternary blends of PP, a polypropylene-grafted acrylic acid copolymer (PP-g-AA), and an ethylene–acrylic acid copolymer (EAA) by melt blending. Scanning electron microscopy observations confirmed that PP-g-AA acted as a compatibilizer and improved the compatibility between PP and EAA in the ternary blends. According to Wang and Ishida [143] the interfacial adhesion of blend of iPP/poly(vinyl methylether) (iPVME) has been improved by the addition of PP-g-AA as a compatibilizing agent. The addition of 2.5 wt% PP-g-AA reduces the PVME domain size greatly and the addition of 5 wt% PP-g-AA results in a homogeneous morphology. The increase of the interfacial adhesion is attributed to the specific intermolecular interaction between the acrylic acid group of PP-g-AA and the ether group of PVME.

Polypropylene–phenol formaldehyde-based compatibilizers, i.e. polypropylene-graft-phenol formaldehyde copolymers (PP-g-PF) were suitable for blends or alloys of PP and engineering polymers having aromatic residues or functionality complimentary to hydroxyl. Blends of iPP/PBT and iPP/poly(phenylene ether) (PPE) were compatibilized by PP-g-PF. Impact strength was observed to be the most sensitive response to blend compatibilization. The PP-g-PF compatibilizer was observed to be more efficient in blends of PBT than of PPE. The main reason for that was the availability of reactive end-groups in the case of PBT, making covalent bonding between the compatibilizer and PBT possible [144].

Thermotropic liquid crystalline ionomer (LCI) is a kind of LCP containing ionic groups; they can offer the possibility for promoting intermolecular interaction through ion–dipole association and the improvement of the interfacial adhesion between the phases in blends. Sun et al. [145] used side-chain liquid crystalline ionomer (SLCI) containing sulfonic acid groups with a polymethylhydrosiloxane main-chain to improve the compatibility of PP and PBT. The SLCI containing sulfonate acid groups acted as physical crosslinking agent along the interface, which compatibilized PP/PBT blends. Specific interaction was formed by ion–dipole interaction between the ionic groups of SLCI and the polar groups in PBT. The interaction led to the compatibilization of the SLCI in PP/PBT/SLCI blends. This resulted in much finer dispersion of the minor PBT phase in PP matrices and stronger interfacial adhesion between these phases. The compatibilization effect of 4 wt% SLCI content was better than that of other SLCI contents in the blends.

PP/PA blends were compatibilized with PP modified with vinylsilane or maleic anhydride and ethylene–propylene random (EPR) copolymer modified with maleic anhydride. Tensile strength and elongation at break increased for blends compatibilized with modified PP. It can be seen that blends compatibilized with PP-g-MAH showed the greatest tensile strength among all the blends. They had the highest elongation at break, indicating good adhesion between the phases. The morphology of the blends showed a finer dispersion of the PA minor phase in the PP matrix [146].

Marco et al. [147] investigated the role played by two different interface agents on the basis of atactic PP in the PP/PA6 blends. Two grafted polymers containing either succinic anhydride (a-PP-SA) or both succinyl-fluorescein and succinic anhydride grafted groups (a-PP-SF/SA). Thermo-optical morphological studies

have indicated that the presence of the interface agents improves the degree of compatibilization through a reduction in the size of the PA6 domains dispersed in the PP matrix. The compatibilizing efficiency of a-PP-SA is greater than that of a-PP-SF/SA for the PP/PA6 system. Franzheim et al. [148] studied the effects of PP-g-MAH on the morphology development of PP/PA6 blends. It was observed that compatibilization has a stronger influence on the blend morphology than a variation of process or rheological conditions with physical blends. Furthermore, the compatibilization leads to a concurrent crystallization of the PA6 phase with the PP phase. According to Laredo et al. [149] the inclusion of 10 wt% of PP-g-MAH into the PP/PA6 (70/30) blend has improved the dispersion of the PA6 in the amorphous phase. Also, the sorption of water of the PP-g-MAH compatibilized PP/PA6 blends is lower than that of the unmodified blend.

Lu et al. [150] prepared amine (primary and secondary) functional PP by the melt blending of maleated PP with small diamines, including hexamethylenediamine (primary–primary diamine), p-xylylenediamine (primary–primary diamine) and N-hexylethylenediamine (primary–secondary diamine), at various diamine/anhydride molar ratios in a batch mixer and a twin-screw extruder. It was found that the adhesion between polyurethane (PU) and PP was greatly promoted by the amine-functionalized PP.

Kim et al. [151] investigated the properties of PP/ethylene vinyl alcohol (EVOH) blends compatibilized with polypropylene grafted with itaconic acid (PP-g-IA). It was found that carboxylic acid groups in PP-g-IA and hydroxyl group in EVOH formed strong in situ hydrogen bond in the compatibilized blends, resulting in better morphological and mechanical properties of the compatibilized blends than those of un-compatibilized blends. In the case of PP/EVOH blends with PP-g-IA, the Young's modulus, ultimate tensile strength and elongation at break increased significantly as compared with PP/EVOH blends without PP-g-IA. These results indicated that PP-g-IA led to a good compatibilizing effect between PP and EVOH resin.

Table 8.1 summarizes some of the compatibilizer used for PP blends. It can be concluded that selection of suitable and loading of compatibilizer is an important factor to enhance the compatibility between PP and other polymers (e.g. PA, PS, ABS, PC, LCP).

8.8.2 Reactive Compatibilization

In the previous section, it can be seen that block copolymers are successfully employed as good compatibilizers because they are able to locate at the interface and act as emulsifiers to lower the interfacial tension. However, due to their high molecular weight nature, large amount of the block copolymers often prefer to form micelles in either homopolymer phases, rather than residing along the interfaces. This make reactive compatibilization an alternative approach to produce useful polymer blends [152].

Table 8.1 Compatibilizer for PP blends (PP as major matrix)

PP type	Other polymer	Compatibilizer	Findings	Reference
Polypropylene (PP) [MW = 590,000 g/mol)	Liquid crystal polymer (LCP; Rodrun LC3000) [60 mol% hydroxybenzoic acid (HBA) and 40 mol% ethylene terephthalate]	PP-g-GMA (glycidyl methacrylate content of 1.5 wt%); loading 1, 2, 5, and 10 wt%	Adding PP-g-GMA further reduced crystallization half-times	[16]
PP	Liquid crystal polymer (LCP)	PP-g-MAH (less than 1 wt% MAH); loading 5 wt%	Adding PP-g-MAH increased tensile modulus, yield stress, yield strain and thermomechanical behavior of PP/LCP blends	[137]
PP	Liquid crystal polymer (LCP)	Ethylene-acrylic acid (EAA) (comonomer content 6 wt%)	Strong interaction formed between the segments of EAA and LCP Vectra A 950 through intermolecular H-bonding in the blends	[136]
PP	Polystyrene (PS)	PP-g-MAH (8 to 10 wt% MAH); loading 2, 5 and 10 wt%	Adding PP-g-MAH stabilizing the morphology and improving the impact strength	[132]
iPP [MW = 3.07×10^5 g/mol]	Atatic polystyrene (PS) [MW = 3.72×10^5 g/mol]	PP-g-PS	PP-g-PS graft copolymers were effective in reducing the PS particle size and enhancing the interfacial adhesion between PP and PS phases	[130]
PP [MW = 230,000 g/mol]	Acrylonitrile butadiene styrene (ABS) [MW = 160,000 g/mol]	SEBS-g-MAH; loading 1, 3, 5, 7 and 10 phr	Adding SEBS-g-MAH (up to 7 phr) improve impact strength of the blends	[138]
iPP	Acrylonitrile-butadiene-styrene (ABS)	PP-g-cardanol (grafting degree is 3.88%); loading 1, 3, 5, 7, 9 phr	Adding PP-g-cardanol improved tensile strength, impact strength and flexural strength of PP/ABS (70/30) blends	[139]

(continued)

Table 8.1 (continued)

PP type	Other polymer	Compatibilizer	Findings	Reference
PP [MW = 386,648 g/mol]	Polycarbonate (PC)	PP-g-BPA (degree of grafting 5.59 BPA); loading 5 and 15 wt%	Adding PP-g-BPA increased tensile strength and impact strength of PP/PC blends	[141]
PP	Ethylene–acrylic acid copolymer (EAA)	PP-g-AA (grafting degree of acrylic acid is 0.85 wt%)	Adding PP-g-AA improved the compatibility between PP and EAA	[142]
iPP [MW = 250,000 g/mol]	Poly(vinyl methylether) (PVME) [MW = 90,000 g/mol]	PP-g-AA (acrylic acid 6 wt%); loading 2.5 and 5 wt%	The addition of 2.5% PP-g-AA reduces the PVME domain size greatly and the addition of 5% PP-g-AA results in a homogeneous morphology	[143]
PP	Polybutylene terephthalate (PBT)	Side-chain liquid crystalline ionomer (SLCI) containing sulfonic acid groups with a polymethylhydrosiloxane main-chain; loading 2–12 wt%	SLCI resulted in much finer dispersion of the minor PBT phase in PP matrices and stronger interfacial adhesion between these phases	[145]
PP	Polyamide 6 (PA6)	PP-g-MAH (functionalization degree MAH 0.70%); loading 4 and 7 wt%	The yield stress and elongation at break of PP/PA6 blends increased significantly	[146]
iPP [MW = 334,000 g/mol]	PA6 [MW = 25,000 g/mol]	Succinic anhydride grafted atactic polypropylene (a-PP-SA) (containing 3.1 wt% grafted groups)	a-PP-SA improved the degree of compatibilization through a reduction in the size of the PA6 domains dispersed in the PP matrix	[147]
PP [MW = 34,400 g/mol]	Ethylene vinyl alcohol (EVOH) [MW= 41,400 g/mol]	PP-g-IA (graft ratio of 1%); loading 10 phr	The PP-g-IA compatibilized PP/EVOH blends have higher storage modulus, Young's moduli, ultimate tensile strength, and elongation at break than un-compatibilized blends	[151]

Hung et al. [152] attempted to reactively compatibilize the nonreactive PP/PS blend system by physically functionalizing PP and PS with the addition of PP-g-MAH and styrene maleic anhydride random copolymer (SMA), respectively. An epoxy monomer, serving as a coupler and possessing four epoxy groups able to react with the maleic anhydride of PP-g-MA and SMA, was added during melt blending. Observations of the finer PS domain sizes and improved mechanical properties support the potential of reactive compatibilization of this nonreactive PP/PS blend by combining physically functionalized PP and PS with tetra-glycidyl ether of diphenyl diamino methane (TGDDM) in a one-step extrusion process. The tensile strength and flexural modulus of the compatibilized blends are substantially improved compared to non-compatibilized blends. A small quantity of the TGDDM is important to function as a coupler in the PP/PS blend during melt blending.

Kaya et al. [153] synthesized oxazoline-functionalized PP by using the *rac*-Et $[1\text{-Ind}]_2ZrCl_2$/Methylaluminoxan (MAO) catalyst system. To investigate their compatibilization efficiency, copolymers with different oxazoline groups were reactive blended with carboxylic-terminated PS. The copolymer with the oxazoline group containing phenoxy moiety showed the highest compatibilization efficiency. The increase in melt viscosity, melting temperature, and onset temperature of the crystallization indicate a reaction between the oxazoline group of the copolymer and the carboxylic group of the PS, resulting in an amide- and an ester-covalent bond. Li et al. [154] prepared isocyanate- and amine-functionalized PP and PS through grafting and copolymerization method. These compounds are used as precursors for PP-g-PS copolymers and reacted at the matrix interface of PP/PS blends. The addition of the reaction compatibilizer greatly altered the distribution in the matrix such that PS particles became finely dispersed. DMA measurements confirm that the compatibility of PP/PS blends with compatibilizers is better than without compatibilizers.

Yang et al. [65] reported that in situ reactive compatibilization of PP and SBS, was achieved in the presence of an initiator, dicumyl peroxide (DCP). Co-vulcanizing agent triallyl isocyanurate (TAIC) was used to improve the crosslinking efficiency from controlling the degradation reaction, remarkably decrease the probability of PP chains scission during blending. With improved interfacial adhesion, compatibilized blends not only were toughened but also exhibited enhanced tensile strength and thermal stability. Cryofractured surface morphologies of reactive compatibilized blends showed a reduction of dispersed particle sizes and an increment on interfacial adhesion, especially for PP/SBS/DCP/TAIC (50/50/1.5/0.75) blend.

Bohn et al. [155] prepared carboxylated and maleated as reactive compatibilizers for PP/PA66 blends. The PP has been functionalized, via reactive extrusion, with MAH and with asymmetric functional peroxide. In compatibilized blends of PP and PA66, the PP that was functionalized with the asymmetric peroxide is found to be an improved compatibilizer compared to that of PP-g-MAH.

Compatible polymer blends of PP with an amorphous polyamide (aPA) were obtained through reactive compatibilization by adding 20 wt% PP-g-MAH to the blends. The aPA was synthesized from a random copolymer of isophthalic acid,

12-aminododecanoic acid, and bis(4-amino-3-methylcyclohexyl) methane. The addition of the compatibilizer to the blends led to both a significant decrease in the dispersed phase particle size (roughly from 1–2 to 0.2 μm) and an improvement in interfacial adhesion. This was attributed to the formation of PP-g-aPA grafted copolymers by an in situ reaction of the anhydride groups of the PP-g-MAH with the amine end groups of aPA as well as to their location at the interface [156].

In Tortorella and Beatty [157] research work, iPP has been reactively blended with various grades of an ethylene–octane copolymer (EOC) in a twin-screw extruder. Free radical polymerization of styrene and a multifunctional acrylate during melt extrusion has resulted in an enhancement of mechanical properties over the binary blend. The reactive blend (containing 74.3% PP, 18.6% EOC, 6% styrene, 0.3 2,5-dimethyl-2,5-di-(t-butylperoxy) hexane initiator, and 0.8% multifunctional acrylate) exhibits a notched Izod impact strength over 12 times that of pure PP and greater than double the performance of the binary blend.

Another possibility for in situ compatibilization of polyolefin/PS blends is an electrophilic substitution of a proton on the aromatic ring of PS by an alkane or olefin in the presence of a strong Lewis acid, known as Friedel–Crafts (F–C) alkylation reaction. Binary polymer blends of PP/PS (blending ratio: 80/20) were compatibilized by Friedel-Crafts alkylation reaction, catalyzed by a Lewis acid of anhydrous aluminum chloride ($AlCl_3$). The results showed that the rheological properties (i.e. storage modulus, loss modulus, complex modulus, and complex viscosity) of the in situ compatiblized blends were all obviously influenced by the rheological properties of the matrix and slightly influenced by the rheological properties of the dispersed phase, especially when $AlCl_3$ content was lower than about 0.10 wt% [158]. Abbasi et al. [159] attempted to study the effect of reactive compatibilization via Friedel–Crafts alkylation reaction, using $AlCl_3$ as a catalyst, on the rheology, morphology and mechanical properties of PP/PS blends in the presence of an organoclay. Generation of PP-g-PS copolymer was confirmed by using FTIR analysis. During the reactive compatibilization process, the interfacial interaction between the PP matrix and dispersed PS phase increased attributed to the formation of PP-g-PS copolymer, which led to finer and well-distributed PS particles in the PP matrix.

8.8.3 Compatibilization Using Nanofiller

The addition of most of the compatibilizers induces a significant loss of blend stiffness. Thus, nanoparticles have then attracted great interest because the nanofiller can play the role of both structural reinforcement and compatibilizer for several types of immiscible polymer blends. It has been proposed that the compatibilizing effect of the nanoparticles on immiscible polymer blends depending on the localisation of the filler in the blend. Yousfi et al. [160] reported that the incorporation of nanoscale talc particles in an immiscible PP/PA6 blends has resulted in remarkable improvements in the morphological structure evidenced by a

dramatic reduction of the dispersed domain size revealed by SEM and transmission electron microscopy (TEM) analysis. The addition of talc nanofillers induces a significant decrease of the size of the PA6 domains.

Graphene oxide (GO) and its derivatives have been employed to compatibilize polymer blends. The π-π stacking effect between graphene (functionalized graphene) and aromatic rings of some polymers can be used to improve the interfacial interaction. A remarkable reduction of interfacial adhesion for an immiscible polymer blend can be achieved by incorporating little amount of graphene. You et al. [161] synthesized polypropylene-graft-reduced graphene oxide (PP-g-rGO) and used as a compatibilizer for PP/PS blends. The PP-g-rGO was prepared by grafting PP-g-MAH chains onto amino functionalized reduced graphene oxide (rGO) nanosheets. SEM observation revealed an obvious reduction of the dispersed PS phase size in PP/PS (70/30 by weight) blends by incorporating only 1.5 wt% of PP-g-rGO. The compatibilization effect of PP-g-rGO lead to the enhancement of the tensile strength and elongation at break of the PP/PS blends. The compatibilizing mechanism is attributed to the fact that PP-g-rGO can adsorb PS chains on their basal planes through π-π stacking, as well as promote intermolecular interactions with PP through the grafted PP chains.

Lin et al. [162] improved the mechanical properties of PP/PET/SEBS-g-MAH blends via selective dispersion of halloysite nanotubes in the blend. The substantially improved mechanical properties in the blends have been correlated to the unique selective dispersion of HNTs in the interfacial region and the changed crystallization behavior. The crystallization of PP in the blend was also facilitated by the selective dispersion of HNTs and the folding surface-free energy was substantially increased.

8.9 Optimization, Modeling and Simulation

8.9.1 Optimization

The optimum condition of processing parameters (mixing temperature, rotor speed, fill factor, and blend ratio) and prediction models for the best key mechanical properties is important to achieve the desired properties of PP blends and suited them for certain application.

Uthaipan et al. [30] investigated the processing and properties EPDM/PP TPV by using the Taguchi's optimization technique and data analysis. The results reveal that all of the processing parameters affected significantly the mechanical properties of the EPDM/PP TPV, but specifically the blend ratio contributed more than 90% in effect size on tensile strength and tension set. It can be summarized that the morphological structure and stress relaxation of the TPVs were strongly governed by the EPDM content in the blend ratio. That is, the higher the EPDM content, the better phase morphology having smaller size of the vulcanized EPDM particles

distributed in the PP matrix and the higher rate of stress relaxation. The influences of processing parameters i.e. mixing temperature, rotor speed, fill factor, and blend ratio on the production of EPDM/PP TPV were statistically investigated, using the Taguchi approach to experiment based optimization. The obtained results suggest that the Taguchi methodology with an L9 orthogonal array as experimental design was successfully used to analyze the effects of processing parameters, and to find optimal sets of parameters for select key mechanical properties of TPVs.

Tucker et al. [163] studied the mechanical and morphological properties of PP/PA6 blends compatibilized with PP-g-MAH and SEBS-g-MAH using a factorial design known as extreme vertices. The effect of PA6/compatibilizer ratio is critical to the optimization of PP/PA6 compatibilized blends irrespective of PA6 amount over the range of compositions studied. The effect is observed in response surfaces of yield stress and modulus for PP-g-MAH compatibilized blends, and SEBS-g-MAH compatibilized blends. The experimental design employed (extreme vertices) is able to effectively use experimental data to model mechanical properties even when very few treatment combinations are used. The quantification of main effects and interactions allows a better understanding of the complex behavior of ternary polymer blends.

8.9.2 Modeling of Flow-Induced Crystallization

Flow-induced crystallization (FIC) is an important experimental phenomenon and is usually observed during polymer processing. FIC leads to specific morphology and mechanical behavior of materials, which are different from those during quiescent crystallization processes. To get an insight into the FIC phenomenon, there has been much work reported concerning the prediction of the crystallization kinetics in a flow field based on different theories. Yu et al. [164] reported the FIC of iPP upon addition of poly(ethylene-co-octene) (PEO) in terms of theoretical modeling. The crystallization of iPP and PEO blends in flow is simulated by a modified FIC model based on the conformation tensor theory. Two kinds of flow fields, shear flow and elongational flow, are considered in the prediction to analyze the influence of flow field on the crystallization kinetics of the polymer. The simulation results show that the elongation flow is much more effective than shear flow in reducing the dimensionless induction time of polymer crystallization. In addition, the induction time of crystallization in the blends is sensitive to the change of shear rate. In comparison with experimental data, the modified model shows its validity for the prediction of the induction time of crystallization of iPP in the blends. The consistency of the experiments and predictions confirmed the validity of the model. The work is helpful to understand the FIC process of iPP in a complex blend system and the rheological properties of iPP/PEO blends.

8.9.3 Molecular Simulation

Molecular simulation has become one of the most important tools to predict or validate structure–property relationship of polyblends, blend compatibility, and phase behavior of polymers. Dai et al. [165] used simulations based on molecular dynamics and MesoDyn theories to investigate the compatibility, morphology evolution of PP/PC blends, and the relationship between the composition and microstructure. The systems of PP/PC (54/46) with larger value of order parameters showed the stronger immiscibility and the faster separation process. The systems of PP/PC (82/18) reached the equilibrium state after a comparatively longer time, and showed less immiscible systems and a slower separation process, which was consistent with the results of free-energy density.

8.10 Conclusion and Future Prospective

This chapter documented the properties and processing of PP blends (e.g. PP/thermoplastic, PP/rubber—TPO and TPV, PP/thermoset, PP/recycled polymers and all-PP blends). The ways to improve the impact toughness and crystallization of PP have been summarized. The compatibility of PP with other polymers can be achieved by using either physical compatibilization or reactive compatibilization. The processing and properties of PP blends should be controlled by design, in order to optimize their performance (e.g. strength, toughness, crystallizability, rheology and morphology). For example, adding compatibilizer may improve the compatibility of the PP blends at the cost of toughness and crystallization; adding elastomer

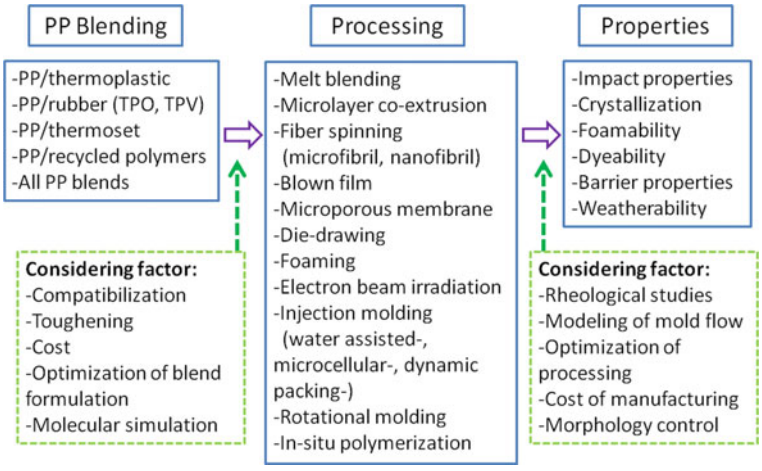

Fig. 8.8 Process and properties control by design for the manufacturing of PP blends

for PP toughening may influencing their compatibility and crystallization behavior; adding "too many" component in PP blends may affecting its rheological behavior and processability. Thus, a proper processing and properties control by design, using advanced modeling and simulation software, together with the strong scientific fundamental background and advanced processing technique should be the way to achieve high performance PP blends. Figure 8.8 shows the process and properties control by design for the manufacturing of PP blends. There are few topics can be considered for the future development of PP blends, these include (1) PP blending with biopolymers using more sustainable processing technique (via green technology), (2) nanoblends based on PP (using nanoscopic morphology stabilization concept), (3) morphology evolution of PP blends via nanofiller compatibilization (through selective dispersion/localization), (4) process-induced phase and crystal morphology development (using nanotechnology), (5) modeling and molecular simulation of the PP blends and (6) in-process morphology control (for example, by using dynamic packing injection molding).

References

1. Zhu Y, Luo F, Bai H et al (2013) Synergistic effects of β-modification and impact polypropylene copolymer on brittle-ductile transition of polypropylene random copolymer. J Appl Polym Sci 129:3613–3622. https://doi.org/10.1002/app.39107
2. Zhang H, Wang J, Cao S, Shan A (2000) Toughened polypropylene with balanced rigidity (I): preparation and chemical structure of toughening master batch. Polym Adv Technol 11:334–341. https://doi.org/10.1002/1099-1581(200007)11:7<334::AID-PAT976>3.0.CO;2-K
3. Chow WS, Abu Bakar A, Mohd Ishak ZA et al (2005) Effect of maleic anhydride-grafted ethylene–propylene rubber on the mechanical, rheological and morphological properties of organoclay reinforced polyamide 6/polypropylene nanocomposites. Eur Polym J 41:687–696. https://doi.org/10.1016/j.eurpolymj.2004.10.041
4. Karger-Kocsis J (2000) Swirl mat- and long discontinuous fiber mat-reinforced polypropylene composites—status and future trends. Polym Compos 21:514–522. https://doi.org/10.1002/pc.10206
5. Zhang RH, Li RKY (2013) Effect of syndiotactic polystyrene on the crystallization behavior of isotactic polypropylene/syndiotactic polystyrene blends with and without β-nucleating agent. Polym Int 62:919–927. https://doi.org/10.1002/pi.4378
6. Lipatov YS (2002) Polymer blends and interpenetrating polymer networks at the interface with solids. Prog Polym Sci 27:1721–1801. https://doi.org/10.1016/S0079-6700(02)00021-7
7. Koning C, Van Duin M, Pagnoulle CJR (1998) Strategies for compatibilization of polymer blends. Prog Polym Sci 23:707–757. https://doi.org/10.1016/s0079-6700(97)00054-3
8. Higgins JS, Tambasco M, Lipson JEG (2005) Polymer blends; stretching what we can learn through the combination of experiment and theory. Prog Polym Sci 30:832–843. https://doi.org/10.1016/j.progpolymsci.2005.06.001
9. He Y, Zhu B, Inoue Y (2004) Hydrogen bonds in polymer blends. Prog Polym Sci 29:1021–1051. https://doi.org/10.1016/j.progpolymsci.2004.07.002
10. Imre B, Renner K, Pukánszky B (2014) Interactions, structure and properties in poly (lactic acid)/thermoplastic polymer blends. Express Polym Lett 8:2–14. https://doi.org/10.3144/expresspolymlett.2014

11. Costa LC, Neto AT, Hage E (2014) PMMA/SAN and SAN/PBT nanoblends obtained by blending extrusion using thermodynamics and microrheology basis. Express Polym Lett 8:164–176. https://doi.org/10.3144/expresspolymlett.2014.20
12. Taguet A, Cassagnau P, Lopez-Cuesta J-M (2014) Progress in polymer science structuration, selective dispersion and compatibilizing effect of (nano) fillers in polymer blends. Prog Polym Sci 39:1526–1563. https://doi.org/10.1016/j.progpolymsci.2014.04.002
13. Chow WS, Mohd Ishak ZA, Karger-Kocsis J et al (2003) Compatibilizing effect of maleated polypropylene on the mechanical properties and morphology of injection molded polyamide 6/polypropylene/organoclay nanocomposites. Polymer 44:7427–7440. https://doi.org/10.1016/j.polymer.2003.09.006
14. Aranburu N, Eguiazábal JI (2015) Improved mechanical properties of compatibilized polypropylene/polyamide-12 blends. Int J Polym Sci 2015:8 pages. https://doi.org/10.1155/2015/742540
15. Zhang Z, Wang C, Du Y et al (2013) Preparation and investigation of the β-nucleated polypropylene/polystyrene blends. J Appl Polym Sci 127:1114–1121. https://doi.org/10.1002/app.37560
16. Acosta MN, Ercoli DR, Goizueta GS et al (2011) Blends of PP/PE co-octene for modified atmosphere packaging applications. Packag Technol Sci 24:223–235. https://doi.org/10.1002/pts.929
17. Gartner C, Suárez M, López BL (2008) Grafting of maleic anhydride on polypropylene and its effect on blending with poly (ethylene terephthalate). Polym Eng Sci 48:1910–1916. https://doi.org/10.1002/pen.21106
18. Yu L, Simon G, Shanks RA, Noblle MR (2000) Crystallization and compatibilization of polypropylene-liquid crystalline polyester blends. J Appl Polym Sci 77:2229–2236. https://doi.org/10.1002/1097-4628(20000906)77:10%3c2229:AID-APP16%3e3.0.CO;2-Z
19. Liang YC, Isayev AI (2002) Self-reinforced polypropylene/lcp extruded strands and their moldings. Polym Eng Sci 42:994–1018. https://doi.org/10.1002/pen.11008
20. Flaris V, Montero N, Steinberg C (2012) Surface energy of polypropylene/polysulfone compatibilized blends. J Vinyl Addit Technol 18:222–227. https://doi.org/10.1002/vnl.20307
21. Yao XR, Wang L, Guo ZX, Yu J (2013) Morphology stabilization of the polypropylene/polystyrene nanoblends prepared by diffusion and polymerization of styrene in isotactic polypropylene pellets during melt mixing by the incorporation of divinylbenzene. J Appl Polym Sci 127:1092–1097. https://doi.org/10.1002/app.37951
22. Öksüz M, Eroğlu M (2005) Effect of the elastomer type on the microstructure and mechanical properties of polypropylene. J Appl Polym Sci 98:1445–1450. https://doi.org/10.1002/app.22271
23. Su Z, Jiang P, Li Q et al (2004) Mechanical properties and morphological structures relationship of blends based on sulfated EPDM ionomer and polypropylene. J Appl Polym Sci 94:1504–1510. https://doi.org/10.1002/app.21068
24. Chakraborty P, Ganguly A, Mitra S, Bhowmick AK (2008) Influence of phase modifiers on morphology and properties of thermoplastic elastomers prepared from ethylene propylene diene rubber and isotactic polypropylene. Polym Eng Sci 48:477–489. https://doi.org/10.1002/pen.20984
25. Ma GQ, Zhao YH, Yan LT et al (2006) Blends of polypropylene with poly(cis-butadiene) rubber. III. Study on the phase structure and morphology of incompatible blends of polypropylene with poly(cis-butadiene) rubber. J Appl Polym Sci 100:4900–4909. https://doi.org/10.1002/app.23499
26. Hristov V, Lach R, Krumova M, Grellmann W (2005) Fracture toughness of modified polypropylene/poly(styrene-ran-butadiene) blends. Polym Int 54:1632–1640. https://doi.org/10.1002/pi.1894
27. Salmah H, Azra BN, Yusrina MD, Ismail H (2015) A comparative study of polypropylene/(chloroprene rubber) and (recycled polypropylene)/(chloroprene rubber) blends. J Vinyl Addit Technol 21:122–127. https://doi.org/10.1002/vnl.21390

28. Karger-Kocsis J, Felhös D, Xu D, Schlarb AK (2008) Unlubricated sliding and rolling wear of thermoplastic dynamic vulcanizates (Santoprene®) against steel. Wear 265:292–300. https://doi.org/10.1016/j.wear.2007.10.010
29. Tanrattanakul V, Kosonmetee K, Laokijcfaaroen P (2009) Polypropylene/natural rubber thermoplastic elastomer: effect of phenolic resin as a vulcanizing agent on mechanical properties and morphology. J Appl Polym Sci 112:3267–3275. https://doi.org/10.1002/app.29816
30. Uthaipan N, Junhasavasdikul B, Nakason C (2015) Prediction models for the key mechanical properties of EPDM/PP blends as affected by processing parameters and their correlation with stress relaxation and phase morphologies 26:970–977. https://doi.org/10.1002/pat.3511
31. Karger-Kocsis J, Kalló A, Kuleznev VN (1984) Phase structure of impact-modified polypropylene blends. Polymer 25:279–286. https://doi.org/10.1016/0032-3861(84)90337-9
32. Jain AK, Nagpal AK, Singhal R, Gupta NK (2000) Effect of dynamic crosslinking on impact strength and other mechanical properties of polypropylene/ethylene-propylene-diene rubber blends. J Appl Polym Sci 78:2089–2103. https://doi.org/10.1002/1097-4628(20001213)78:12%3c2089:AID-APP50%3e3.0.CO;2-H
33. Gupta NK, Jain AK, Singhal R, Nagpal AK (2000) Effect of dynamic crosslinking on tensile yield behavior of polypropylene/ethylene-propylene-diene rubber blends. J Appl Polym Sci 78:2104–2121. https://doi.org/10.1002/1097-4628(20001213)78:12%3c2104:AID-APP60%3e3.0.CO;2-7
34. Naskar K, Gohs U, Wagenknecht U, Heinrich G (2009) PP-EPDM thermoplastic vulcanisates (TPVs) by electron induced reactive processing. Express Polym Lett 3:677–683. https://doi.org/10.3144/expresspolymlett.2009.85
35. Nakason C, Wannavilai P, Kaesaman A (2006) Thermoplastic vulcanizates based on epoxidized natural rubber/polypropylene blends: effect of compatibilizers and reactive blending. J Appl Polym Sci 100:4729–4740. https://doi.org/10.1002/app.23260
36. Nakason C, Wannavilai P, Kaesaman A (2005) Thermoplastic vulcanizates based on epoxidized natural rubber/polypropylene blends: effect of epoxide levels in ENR molecules. J Appl Polym Sci 101:3046–3052. https://doi.org/10.1002/app.23926
37. Verbois A, Cassagnau P, Michel A et al (2004) New thermoplastic vulcanizate, composed of polypropylene and ethylene-vinyl acetate copolymer crosslinked by tetrapropoxysilane: evolution of the blend morphology with respect to the crosslinking reaction conversion. Polym Int 53:523–535. https://doi.org/10.1002/pi.1428
38. Soares BG, De Oliveira M, Meireles D et al (2008) Dynamically vulcanized polypropylene/nitrile rubber blends: the effect of peroxide/bis-maleimide curing system and different compatibilizing systems. J Appl Polym Sci 110:3566–3573. https://doi.org/10.1002/app.28946
39. Van Dyke JD, Gnatowski M, Burczyk A (2008) Solvent resistance and mechanical properties in thermoplastic elastomer blends prepared by dynamic vulcanization. J Appl Polym Sci 109:1535–1546. https://doi.org/10.1002/app.28149
40. Mandal AK, Siddhanta SK, Chakraborty D (2013) Chlorosulfonated polyethylene-polypropylene thermoplastic vulcanizate: mechanical, morphological, thermal, and rheological properties. J Appl Polym Sci 127:1268–1274. https://doi.org/10.1002/app.37725
41. Babu RR, Singha NK, Naskar K (2010) Dynamically vulcanized blends of polypropylene and ethylene octene copolymer: influence of various coagents on thermal and rheological characteristics. J Appl Polym Sci 117:1578–1590. https://doi.org/10.1002/app.32023
42. Wan C, Patel SH, Xanthos M (2003) Reactive melt modification of polypropylene with a crosslinkable polyester. Polym Eng Sci 43:1276–1288. https://doi.org/10.1002/pen.10108
43. Jiang X, Huang H, Zhang Y, Zhang Y (2004) Dynamically cured polypropylene/epoxy blends. J Appl Polym Sci 92:1437–1448. https://doi.org/10.1002/app.13700
44. Cui L, Zhou Z, Zhang Y et al (2007) Rheological behavior of polypropylene/novolac blends. J Appl Polym Sci 106:811–816. https://doi.org/10.1002/app.26515

45. Phillips RA (2000) Macromorphology of polypropylene homopolymer tacticity mixtures. J Polym Sci, Part B: Polym Phys 38:1947–1964. https://doi.org/10.1002/1099-0488(20000801)38:15%3c1947:AID-POLB10%3e3.0.CO;2-M
46. Flores-Gallardo SG, Sánchez-Valdes S, Ramos De Valle LF (2001) Polypropylene/polypropylene-grafted acrylic acid blends for multilayer films: preparation and characterization. J Appl Polym Sci 79:1497–1505. https://doi.org/10.1002/1097-4628(20010222)79:8%3c1497:AID-APP170%3e3.0.CO;2-3
47. Saffar A, Jalali Dil E, Carreau PJ et al (2016) Phase behavior of binary blends of PP/PP-g-AA: limitations of the conventional characterization techniques. Polym Int 65:508–515. https://doi.org/10.1002/pi.5082
48. Moya EL, Van Grieken R, Carrero A, Paredes B (2012) Bimodal poly(propylene) through binary metallocene catalytic systems as an alternative to melt blending. Macromol Symp 321–322:46–52. https://doi.org/10.1002/masy.201251107
49. Fang Y, Sadeghi F, Fleuret G, Carreau PJ (2008) Properties of blends of linear and branched polypropylenes in film blowing. Can J Chem Eng 86:6–14. https://doi.org/10.1002/cjce.20011
50. Miskolczi N, Kucharczyk P, Sedlarik V, Szakacs H (2013) Plastic waste minimization: compatibilization of polypropylene/polyamide 6 blends by polyalkenyl-poly-maleic-anhydride-based agents. J Appl Polym Sci 129:3028–3037. https://doi.org/10.1002/app.38724
51. Garcia PS, Gouveia RF, Maia JM et al (2018) 2D and 3D imaging of the deformation behavior of partially devulcanized rubber/polypropylene blends. Express Polym Lett 12:1047–1060. https://doi.org/10.3144/expresspolymlett.2018.92
52. Inoya H, Wei Leong Y, Klinklai W et al (2012) Compatibilization of recycled poly(ethylene terephthalate) and polypropylene blends: effect of polypropylene molecular weight on homogeneity and compatibility. J Appl Polym Sci 124:3947–3955. https://doi.org/10.1002/app.34405
53. Barhoumi N, Jaziri M, Massardier V, Cassagnau P (2008) Valorization of poly(butylene terephthalate) wastes by blending with virgin polypropylene: effect of the composition and the compatibilization. Polym Eng Sci 48:1592–1599. https://doi.org/10.1002/pen.21116
54. Kukaleva N, Simon GP, Kosior E (2003) Binary and ternary blends of recycled high-density polyethylene containing polypropylenes. Polym Eng Sci 43:431–443. https://doi.org/10.1002/pen.10035
55. Kazemi Y, Ramezani Kakroodi A, Rodrigue D (2015) Compatibilization efficiency in post-consumer recycled polyethylene/polypropylene blends: effect of contamination. Polym Eng Sci 55:2368–2376. https://doi.org/10.1002/pen.24125
56. Jaziri M, Barhoumi N, Massardier V, Mélis F (2008) Blending PP with PA6 industrial wastes: effect of the composition and the compatibilization. J Appl Polym Sci 107:3451–3458. https://doi.org/10.1002/app.27542
57. Tchomakov KP, Favis BD, Huneault MA et al (2005) Mechanical properties and morphology of ternary PP/EPDM/PE blends. Can J Chem Eng 83:300–309. https://doi.org/10.1002/cjce.5450830216
58. Vranjes N, Rek V (2007) Effect of EPDM on morphology, mechanical properties, crystallization behavior and viscoelastic properties of iPP + HDPE blends. Macromol Symp 258:90–100. https://doi.org/10.1002/masy.200751210
59. Panda B, Bhattacharyya AR, Kulkarni AR (2013) Morphology and dielectric relaxation spectroscopy of ternary polymer blends of polyamide6, polypropylene, and acrylonitrile butadiene styrene co-polymer: Influence of compatibilizer and multiwall carbon nanotubes. J Appl Polym Sci 127:1433–1445. https://doi.org/10.1002/app.38074
60. Lima PS, Oliveira JM, Costa VAF (2015) Partial replacement of EPR by GTR in highly flowable PP/EPR blends: effects on morphology and mechanical properties. J Appl Polym Sci 132:42011 (1–9). https://doi.org/10.1002/app.42011

61. Debout MA, Robertson RE (2004) Impact strength and elongation-to-break of compatibilized ternary blends of polypropylene, nylon 66, and polystyrene. Polym Eng Sci 44:1800–1809. https://doi.org/10.1002/pen.20182
62. Šmit I, Radonjič G (2000) Effects of SBS on phase morphology of iPP/aPS blends. Polym Eng Sci 40:2144–2160. https://doi.org/10.1002/pen.11347
63. Jazani OM, Arefazar A, Jafari SH et al (2011) A study on the effects of SEBS-g-MAH on the phase morphology and mechanical properties of polypropylene/polycarbonate/SEBS ternary polymer blends. J Appl Polym Sci 121:2680–2687. https://doi.org/10.1002/app.33715
64. Chand N, Naik AM, Khaira HK (2007) Development of UHMWPE modified PP/PET blends and their mechanical and abrasive wear behavior. Polym Compos 28:267–272. https://doi.org/10.1002/pc.20302
65. Yang L, Huang J, Lu X et al (2015) Influences of dicumyl peroxide on morphology and mechanical properties of polypropylene/poly(styrene-b-butadiene-b-styrene) blends via vane-extruder. J Appl Polym Sci 132:41543 (1–12). https://doi.org/10.1002/app.41543
66. Jia S, Qu J, Liu W et al (2014) Thermoplastic polyurethane/polypropylene blends based on novel vane extruder: a study of morphology and mechanical properties. Polym Eng Sci 54:716–724. https://doi.org/10.1002/pen.23598
67. Qu JP, Chen HZ, Liu SR et al (2013) Morphology study of immiscible polymer blends in a vane extruder. J Appl Polym Sci 128:3576–3585. https://doi.org/10.1002/app.38573
68. Shon K, Bumm SH, White JL (2008) A comparative study of dispersing a polyamide 6 into a polypropylene melt in a buss kneader, continuous mixer, and modular intermeshing corotating and counter-rotating twin screw extruders. Polym Eng Sci 48:755–766. https://doi.org/10.1002/pen.20941
69. Polaskova M, Cermak R, Sedlacek T et al (2010) Extrusion of polyethylene/polypropylene blends with microfibrillar-phase morphology. Polym Compos 31:1427–1433. https://doi.org/10.1002/pc.20928
70. Wang K, Zhou C, Zhang H, Zhao D (2002) Modification of polypropylene by melt vibration blending with ultra high molecular weight polyethylene. Adv Polym Technol 21:164–176. https://doi.org/10.1002/adv.10020
71. Tortorella N, Beatty CL (2008) Morphology and crystalline properties of impact-modified polypropylene blends. Polym Eng Sci 48:1476–1486. https://doi.org/10.1002/pen.21102
72. Teng J, Otaigbe JU, Taylor EP (2004) Reactive blending of functionalized polypropylene and polyamide 6: in situ polymerization and in situ compatibilization. Polym Eng Sci 44:648–659. https://doi.org/10.1002/pen.20059
73. Godshall D, White C, Wilkes GL (2001) Effect of compatibilizer molecular weight and maleic anhydride content on interfacial adhesion of polypropylene-PA6 bicomponent fibers. J Appl Polym Sci 80:130–141. https://doi.org/10.1002/1097-4628(20010411)80:2%3c130:AID-APP1081%3e3.0.CO;2-C
74. Fallahi E, Barmar M, Kish MH (2008) Micro and nano fibrils from polypropylene/nylon 6 blends. J Appl Polym Sci 108:1473–1481. https://doi.org/10.1002/app.27792
75. Soroudi A, Skrifvars M (2012) Electroconductive polyblend fibers of polyamide-6/polypropylene/ polyaniline: electrical, morphological, and mechanical characteristics. Polym Eng Sci 52:1606–1612. https://doi.org/10.1002/pen.23074
76. Auinger T, Stadlbauer M (2010) Inter-relationship between processing conditions and mechanical properties of blown film from different polypropylenes and high melt strength polypropylene blends. J Appl Polym Sci 117:155–162. https://doi.org/10.1002/app.31928
77. Jarus D, Hiltner A, Baer E (2001) Microlayer coextrusion as a route to innovative blend structures. Polym Eng Sci 41:2162–2171. https://doi.org/10.1002/pen.10911
78. Xanthos M, Chandavasu C, Sirkar KK, Gogos CG (2002) Melt processed microporous films from compatibilized immiscible blends with potential as membranes. Polym Eng Sci 42:810–825. https://doi.org/10.1002/pen.10993
79. Sadeghi F, Ajji A, Carreau PJ (2008) Microporous membranes obtained from polypropylene blends with superior permeability properties. J Polym Sci, Part B: Polym Phys 46:148–157. https://doi.org/10.1002/polb.21350

80. Ait-Kadi A, Bousmina M, Yousefi AA, Mighri F (2007) High performance structured polymer barrier films obtained from compatibilized polypropylene/ethylene vinyl alcohol blends. Polym Eng Sci 47:1114–1121. https://doi.org/10.1002/pen.20794
81. Mohanraj J, Chapleau N, Ajji A et al (2003) Production, properties and impact toughness of die-drawn toughened polypropylenes. Polym Eng Sci 43:1317–1336. https://doi.org/10.1002/Pen.10112
82. Mondal M, Gohs U, Wagenknecht U, Heinrich G (2013) Efficiency of high energy electrons to produce polypropylene/natural rubber-based thermoplastic elastomer. Polym Eng Sci 53:1696–1705. https://doi.org/10.1002/pen.23414
83. Ali ZI, Youssef HA, Said HM, Saleh HH (2006) Influence of electron beam irradiation and polyfunctional monomer loading on the physico-chemical properties of polyethylene/polypropylene blends. Adv Polym Technol 25:208–217. https://doi.org/10.1002/adv.20072
84. Wang M, Ma J, Chu R et al (2012) Effect of the introduction of polydimethylsiloxane on the foaming behavior of block-copolymerized polypropylene. J Appl Polym Sci 123:2726–2732. https://doi.org/10.1002/app.34854
85. Zhang P, Zhou NQ, Wu QF et al (2007) Microcellular foaming of PE/PP blends. J Appl Polym Sci 104:4149–4159. https://doi.org/10.1002/app.26071
86. Spitael P, Macosko CW (2004) Strain hardening in polypropylenes and its role in extrusion foaming. Polym Eng Sci 44:2090–2100. https://doi.org/10.1002/pen.20214
87. Wang B, Huang HX, Wang ZY (2015) Process-induced phase and crystal morphologies in water-assisted injection molded polypropylene/polymeric β-nucleating agent blend parts. Polym Eng Sci 55:1698–1705. https://doi.org/10.1002/pen.24008
88. Wang WQ, Kontopoulou M (2004) Rotational molding of polypropylene/ultra-low-density ethylene-α-olefin copolymer blends. Polym Eng Sci 44:1662–1669. https://doi.org/10.1002/pen.20165
89. Pires M, Mauler RS, Liberman SA (2004) Structural characterization of reactor blends of polypropylene and ethylene-propylene rubber. J Appl Polym Sci 92:2155–2162. https://doi.org/10.1002/app.20193
90. Liu T, Lei Y, Chen Z et al (2015) Effects of processing conditions on foaming behaviors of polyetherimide (PEI) and PEI/polypropylene blends in microcellular injection molding process. J Appl Polym Sci 132:41443. https://doi.org/10.1002/app.41443
91. Su R, Jiang K, Ge Y et al (2011) Shear-induced fibrillation and resultant mechanical properties of injection-molded polyamide 1010/isotactic polypropylene blends. Polym Int 60:1655–1662. https://doi.org/10.1002/pi.3148
92. Tang J, Tang W, Yuan H, Jin R (2010) Super-toughed polymer blends derived from polypropylene random copolymer and ethylene/styrene interpolymer. J Appl Polym Sci 115:190–197. https://doi.org/10.1002/app.31035
93. Tang W, Tang J, Yuan H, Jin R (2011) Crystallization behavior and mechanical properties of polypropylene random copolymer/poly(ethylene-octene) blends. J Appl Polym Sci 122:461–468. https://doi.org/10.1002/app.34162
94. Li X, Su R, Gao J et al (2011) Toughening of polypropylene with crystallizable poly(ethylene oxide). Polym Int 60:781–786. https://doi.org/10.1002/pi.3015
95. Kakkar D, Maiti SN (2012) Effect of flexibility of ethylene vinyl acetate and crystallization of polypropylene on the mechanical properties of i-PP/EVA blends. J Appl Polym Sci 123:1905–1912. https://doi.org/10.1002/app.34680
96. Premphet K, Paecharoenchai W (2002) Polypropylene/metallocene ethylene-octene copolymer blends with a bimodal particle size distribution: mechanical properties and their controlling factors. J Appl Polym Sci 85:2412–2418. https://doi.org/10.1002/app.10886
97. Thanyaprueksanon S, Thongyai S, Praserthdam P (2007) New synthesis methods for polypropylene-co-ethylene-propylene rubber. J Appl Polym Sci 103:3609–3616. https://doi.org/10.1002/app.25392
98. Liu G, Zhang X, Li X et al (2012) Correlation of miscibility and mechanical properties of polypropylene/olefin block copolymers: effect of chain composition. J Appl Polym Sci 125:666–675. https://doi.org/10.1002/app.36244

99. Bai H, Wang Y, Song B, Han L (2008) Synergistic toughening effects of nucleating agent and ethylene–octene copolymer on polypropylene. J Appl Polym Sci 108:3270–3280. https://doi.org/10.1002/app
100. Fanegas N, Gómez MA, Jiménez I et al (2008) Optimizing the balance between impact strength and stiffness in polypropylene/elastomer blends by incorporation of a nucleating agent. Polym Eng Sci 48:80–87. https://doi.org/10.1002/pen.20886
101. Grein C, Gahleitner M (2008) On the influence of nucleation on the toughness of iPP/EPR blends with different rubber molecular architectures. Express Polym Lett 2:392–397. https://doi.org/10.3144/expresspolymlett.2008.47
102. Jafari SH, Gupta AK (2000) Impact strength and dynamic mechanical properties correlation in elastomer-modified polypropylene. J Appl Polym Sci 78:962–971. https://doi.org/10.1002/1097-4628(20001031)78:5%3c962:AID-APP40%3e3.0.CO;2-5
103. Varga J (1995) Crystallization, melting and supermolecular structure of isotactic polypropylene. Polypropylene structure, blends and composites. Springer, Netherlands, Dordrecht, pp 56–115
104. Chen HB, Karger-Kocsis J, Wu JS, Varga J (2002) Fracture toughness of α- and β-phase polypropylene homopolymers and random- and block-copolymers. Polymer 43:6505–6514. https://doi.org/10.1016/S0032-3861(02)00590-6
105. Wang ZG, Phillips RA, Hsiao BS (2001) Morphology development during isothermal crystallization. II. Isotactic and syndiotactic polypropylene blends. J Polym Sci, Part B: Polym Phys 39:1876–1888. https://doi.org/10.1002/polb.1162
106. Finlay J, Hill MJ, Barham PJ et al (2003) Mechanical properties and characterization of slowly cooled isotactic polypropylene/high-density polyethylene blends. J Polym Sci, Part B: Polym Phys 41:1384–1392. https://doi.org/10.1002/polb.10440
107. Borysiak S (2011) The supermolecular structure of isotactic polypropylene/atactic polystyrene blends. Polym Eng Sci 51:2505–2516. https://doi.org/10.1002/pen.22039
108. Yang J, White JL (2012) Crystallization behavior of polypropylene/ethylene butene copolymer blends. J Appl Polym Sci 126:2049–2058. https://doi.org/10.1002/app.35184
109. Zhang Y, Huang Y, Mai K (2005) Crystallization and dynamic mechanical properties of polypropylene/polystyrene blends modified with maleic anhydride and styrene. J Appl Polym Sci 96:2038–2045. https://doi.org/10.1002/app.21658
110. Yang Z, Zhang Z, Tao Y, Mai K (2009) Preparation, crystallization behavior, and melting characteristics of β-nucleated isotactic polypropylene blends with polyamide. 112:1–8. https://doi.org/10.1002/app
111. Marinelli AL, Bretas RES (2002) Blends of polypropylene resins with a liquid crystalline polymer. I. Isothermal crystallization. J Appl Polym Sci 87:916–930. https://doi.org/10.1002/app.11386
112. Guan Y, Wang S, Zheng A, Xiao H (2003) Crystallization behaviors of polypropylene and functional polypropylene. J Appl Polym Sci 88:872–877. https://doi.org/10.1002/app.11668
113. Wu Y, Yang Y, Li B, Han Y (2006) Reactive blending of modified polypropylene and polyamide 12: effects of compatibilizer content on crystallization and blend morphology. J Appl Polym Sci 100:3187–3192. https://doi.org/10.1002/app.23572
114. Wang D, Gao J (2006) Melting, nonisothermal crystallization behavior and morphology of polypropylene/random ethylene-propylene copolymer blends. J Appl Polym Sci 99:670–678. https://doi.org/10.1002/app.22507
115. Lin Z, Chen C, Li B et al (2012) Compatibility, morphology, and crystallization behavior of compatibilized β-nucleated polypropylene/poly(trimethylene terephthalate) blends. J Appl Polym Sci 125:1616–1624. https://doi.org/10.1002/app.35635
116. Hao XQ, Zheng GQ, Dai K et al (2011) Facile preparation of rich β-transcrystallinity in PET fiber/iPP composites. Express Polym Lett 5:1017–1026. https://doi.org/10.3144/expresspolymlett.2011.99
117. Lima PS, Oliveira JM, Costa VAF (2015) Crystallization kinetics of thermoplastic elastomeric blends based on ground tyre rubber. J Appl Polym Sci 132:42589 (1–11). https://doi.org/10.1002/app.42589

118. Paul S, Kale DD (2002) Rheological study of polypropylene copolymer/polyolefinic elastomer blends. J Appl Polym Sci 84:665–671. https://doi.org/10.1002/app.10376
119. Zhang XM, Li H, Chen WX, Feng LF (2012) Rheological properties and morphological evolutions of polypropylene/ethylene-butene copolymer blends. Polym Eng Sci 52:1740–1748. https://doi.org/10.1002/pen.23116
120. López Manchado MA, Biagiotti J, Kenny JM (2001) Rheological behavior and processability of polypropylene blends with rubber ethylene propylene diene terpolymer. J Appl Polym Sci 81:1–10. https://doi.org/10.1002/app.1407
121. Ardakani F, Jahani Y, Morshedian J (2012) Dynamic viscoelastic behavior of polypropylene/polybutene-1 blends and its correlation with morphology. J Appl Polym Sci 125:640–648. https://doi.org/10.1002/app.36324
122. Marguerat F, Carreau PJ, Michel A (2002) Morphology and rheological properties of polypropylene/reactive elastomer blends. Polym Eng Sci 42:1941–1955. https://doi.org/10.1002/pen.11087
123. Shi D, Jiang F, Ke Z et al (2006) Melt rheological properties of polypropylene-polyamide6 blends compatibilized with maleic anhydride-grafted polypropylene. Polym Int 55:701–707. https://doi.org/10.1002/pi.2036
124. Liao HY, Zheng LY, Hu YB et al (2015) Dynamic rheological behavior of reactively compatibilized polypropylene/polyamide 6 blending melts. J Appl Polym Sci 132:42091 (1–8). https://doi.org/10.1002/app.42091
125. Li Z, Chen M, Ma W (2016) Promoting effect of crystallization on the foaming behavior in polypropylene homopolymer/polypropylene block copolymer blends. Polym Eng Sci 56:1175–1181. https://doi.org/10.1002/pen.24351
126. Laguna-Gutierrez E, Van Hooghten R, Moldenaers P, Rodriguez-Perez MA (2015) Understanding the foamability and mechanical properties of foamed polypropylene blends by using extensional rheology. J Appl Polym Sci 132:42430 (1–14). https://doi.org/10.1002/app.42430
127. Mirjalili F, Moradian S, Ameri F (2011) Attaining optimal dyeability and tensile properties of polypropylene/poly(ethylene terephthalate) blends with a special cubic mixture experimental design. J Appl Polym Sci 121:3201–3210. https://doi.org/10.1002/app.33859
128. Mouffok S, Kaci M (2015) Artificial weathering effect on the structure and properties of polypropylene/polyamide-6 blends compatibilized with PP-g-MA. J Appl Polym Sci 132. https://doi.org/10.1002/app.41722
129. Jose S, Francis B, Thomas S, Karger-Kocsis J (2006) Morphology and mechanical properties of polyamide 12/polypropylene blends in presence and absence of reactive compatibiliser. Polymer 47:3874–3888. https://doi.org/10.1016/j.polymer.2006.03.046
130. Wang L, Tan H, Gong J, Tang T (2014) Relationship between branch length and the compatibilizing effect of polypropylene-g-polystyrene graft copolymer on polypropylene/polystyrene blends. J Appl Polym Sci 131:40126 (1–9). https://doi.org/10.1002/app.40126
131. Li Z, Ke Y, Hu Y (2004) Study on a new kind of polypropylene-graft-polystyrene: preparation and application. J Appl Polym Sci 93:314–322. https://doi.org/10.1002/app.20472
132. Parameswaranpillai J, Joseph G, Jose S, Hameed N (2015) Phase morphology, thermomechanical, and crystallization behavior of uncompatibilized and PP-g-MAH compatibilized polypropylene/polystyrene blends. J Appl Polym Sci 132:42100 (1–11). https://doi.org/10.1002/app.42100
133. Slouf M, Radonjic G, Hlavata D, Sikora A (2006) Compatibilized iPP/aPS blends: the effect of the viscosity ratio of the components on the blends morphology. J Appl Polym Sci 101:2236–2249. https://doi.org/10.1002/app.23571
134. Syed Mustafa SJ, Azlan MRN, Fuad MYA et al (2001) Polypropylene/polystyrene blends-preliminary studies for compatibilization by aromatic-grafted polypropylene. J Appl Polym Sci 82:428–434. https://doi.org/10.1002/app.1868
135. Mandal PK, Chakraborty D (2009) Studies on morphology, mechanical, thermal, and dynamic mechanical behavior of extrusion blended polypropylene and thermotropic liquid

crystalline polymer in presence of compatibilizer. J Appl Polym Sci 111:2345–2352. https://doi.org/10.1002/app.28988
136. Mandal PK, Siddhanta SK, Chakraborty D (2012) Engineering properties of compatibilized polypropylene/liquid crystalline polymer blends. J Appl Polym Sci 124:5279–5285. https://doi.org/10.1002/app.34277
137. Farasoglou P, Kontou E, Spathis G et al (2000) Processing conditions and compatibilizing effects on reinforcement of polypropylene-liquid crystalline polymer blends. Polym Compos 21:84–95. https://doi.org/10.1002/pc.10167
138. Lee YK, Lee JB, Park DH, Kim WN (2013) Effects of accelerated aging and compatibilizers on the mechanical and morphological properties of polypropylene and poly (acrylonitrile-butadiene-styrene) blends. J Appl Polym Sci 127:1032–1037. https://doi.org/10.1002/app.37504
139. Deng Y, Mao X, Lin J, Chen Q (2015) Compatibilization of polypropylene/poly (acrylonitrile-butadiene-styrene) blends by polypropylene-graft-cardanol. J Appl Polym Sci 132:41315 (1–7). https://doi.org/10.1002/APP.41315
140. Lee HS, Kim JD (2012) Effect of a hybrid compatibilizer on the mechanical properties and interfacial tension of a ternary blend with polypropylene, poly(lactic acid), and a toughening modifier. Polym Compos 33:1154–1161. https://doi.org/10.1002/pc.22244
141. Dai S, Ye L (2008) Effect of novel compatibilizers on the properties and morphology of PP/PC blends. Polym Adv Technol 19:1069–1076. https://doi.org/10.1002/pat.1080
142. Zhang J, Yao Y, Wang XL, Xu JH (2006) Polypropylene/polypropylene-grafted acrylic acid copolymer/ethylene-acrylic acid copolymer ternary blends for hydrophilic polypropylene. J Appl Polym Sci 101:436–442. https://doi.org/10.1002/app.23252
143. Wang D, Ishida H (2006) The effect of addition of poly(propylene-g-acrylic acid) on the morphology of poly(vinyl methylether) and isotactic polypropylene blend. J Appl Polym Sci 101:4098–4103. https://doi.org/10.1002/app.23429
144. Børve KL, Kotlar HK, Gustafson C-G (2000) Polypropylene-phenol formaldehyde-based compatibilizers. III. Application in PP/PBT and PP/PPE blends. J Appl Polym Sci 75:361–370. https://doi.org/10.1002/(SICI)1097-4628(20000118)75:3%3c361:AID-APP4%3e3.0.CO;2-A
145. Sun QJ, Zhang BY, Yao DS et al (2009) Miscibility enhancement of PP/PBT blends with a side-chain liquid crystalline ionomer. J Appl Polym Sci 112:3007–3015. https://doi.org/10.1002/app.29874
146. Nachtigall SMB, Felix AHO, Mauler RS (2003) Blend compatibilizers based on silane- and maleic anhydride-modified polyolefins. J Appl Polym Sci 88:2492–2498. https://doi.org/10.1002/app.12119
147. Marco C, Collar EP, Areso S, García-Martínez JM (2002) Thermal studies on polypropylene/polyamide-6 blends modified by succinic anhydride and succinyl fluorescein grafted polypropylenes. J Polym Sci B: Polym Phys 40:1307–1315. https://doi.org/10.1002/polb.10188
148. Franzheim O, Rische T, Stephan M, Macknight WJ (2000) Blending of immiscible polymers in a mixing zone of a twin screw extruder—effects of compatibilization. Polym Eng Sci 40:1143–1156. https://doi.org/10.1002/pen.11242
149. Laredo E, Grimau M, Bello A et al (2005) The effect of compatibilization on the dynamic properties of polypropylene/nylon-6 blends studied by broad band dielectric spectroscopy. J Polym Sci B: Polym Phys 43:1408–1420. https://doi.org/10.1002/polb.20421
150. Lu QW, Macosko CW, Horrion J (2005) Melt amination of polypropylenes. J Polym Sci A: Polym Chem 43:4217–4232. https://doi.org/10.1002/pola.20899
151. Kim JS, Jang JH, Kim JH et al (2016) Morphological, thermal, rheological, and mechanical properties of PP/EVOH blends compatibilized with PP-g-IA. Polym Eng Sci 56:1240–1247. https://doi.org/10.1002/pen.24357
152. Hung CJ, Chuang HY, Chang FC (2008) Novel reactive compatibilization strategy on immiscible polypropylene and polystyrene blend. J Appl Polym Sci 107:831–839. https://doi.org/10.1002/app.25201

153. Kaya A, Pompe G, Schulze U et al (2002) The effect of TIBA on metallocene/MAO catalyzed synthesis of propylene oxazoline copolymers and their use in reactive blending. J Appl Polym Sci 86:2174–2181. https://doi.org/10.1002/app.11161
154. Li H, Zhang XM, Zhu SY et al (2015) Preparation of polypropylene and polystyrene with -NCO and -NH_2 functional groups and their applications in polypropylene/polystyrene blends. Polym Eng Sci 55:614–623. https://doi.org/10.1002/pen.23927
155. Bohn CC, Manning SC, Moore RB (2001) Comparison of carboxylated and maleated polypropylene as reactive compatibilizers in polypropylene/polyamide-6,6 blends. J Appl Polym Sci 79:2398–2407. https://doi.org/10.1002/1097-4628(20010328)79:13%3c2398:AID-APP1047%3e3.0.CO;2-3
156. Aranburu N, Eguiazabal JI (2013) Compatible blends of polypropylene with an amorphous polyamide. J Appl Polym Sci 127:5007–5013. https://doi.org/10.1002/app.38090
157. Tortorella N, Beatty CL (2008) Morphology and mechanical properties of impact modified polypropylene blends. Polym Eng Sci 48:2098–2110. https://doi.org/10.1002/pen.21089
158. Li J, Ma G, Sheng J (2010) Linear viscoelastic characteristics of in situ compatiblized binary polymer blends with viscoelastic properties of components variable. J Polym Sci, Part B: Polym Phys 48:1349–1362. https://doi.org/10.1002/polb.22034
159. Abbasi F, Tavakoli A, Razavi Aghjeh MK (2018) Rheology, morphology, and mechanical properties of reactive compatibilized polypropylene/polystyrene blends via Friedel-Crafts alkylation reaction in the presence of clay. J Vinyl Addit Technol 24:18–26. https://doi.org/10.1002/vnl.21522
160. Yousfi M, Livi S, Dumas A et al (2014) Compatibilization of polypropylene/polyamide 6 blends using new synthetic nanosized talc fillers: Morphology, thermal, and mechanical properties. J Appl Polym Sci 131:40453 (1–12). https://doi.org/10.1002/app.40453
161. You F, Wang D, Li X et al (2014) Synthesis of polypropylene-grafted graphene and its compatibilization effect on polypropylene/polystyrene blends. J Appl Polym Sci 131:40455 (1–7). https://doi.org/10.1002/app.40455
162. Lin T, Zhu L, Chen T, Guo B (2013) Optimization of mechanical performance of compatibilized polypropylene/poly(ethylene terephthalate) blends via selective dispersion of halloysite nanotubes in the blend. J Appl Polym Sci 129:47–56. https://doi.org/10.1002/app.38700
163. Tucker JD, Lee S, Einsporn RL (2000) Study of the effect of PP-g-MA and SEBS-g-MA on the mechanical and morphological properties of polypropylene/nylon 6 blends. Polym Eng Sci 40:2577–2589. https://doi.org/10.1002/pen.11388
164. Yu F, Zhang Z, Yu W et al (2012) Modeling of flow-induced crystallization in blends of isotactic polypropylene and poly(ethylene-co-octene). Polym Int 61:1389–1393. https://doi.org/10.1002/pi.4220
165. Dai S, Ye L, Hu GH (2012) Molecular simulation on relationship between composition and microstructure of PP/PC blend. J Appl Polym Sci 126:1165–1173. https://doi.org/10.1002/app.36977